Over then Under Tangles

Dror Bar-Natan
Department of Mathematics
University of Toronto
Toronto Ontario M5S 2E4, Canada
drorbn@math.toronto.edu and *http://www.math.toronto.edu/drorbn*

Zsuzsanna Dancso
School of Mathematics and Statistics
The University of Sydney
Eastern Ave, Camperdown NSW 2006, Australia
zsuzsanna.dancso@sydney.edu.au and *http://zsuzsannadancso.net*

Roland van der Veen
University of Groningen, Bernoulli Institute
P.O. Box 407
9700 AK Groningen, The Netherlands
roland.mathematics@gmail.com and *http://www.rolandvdv.nl/*

ABSTRACT

Over-then-Under (OU) tangles are oriented tangles whose strands travel through all of their over crossings before any under crossings. In this paper we discuss the idea of *gliding*: an algorithm by which tangle diagrams could be brought to OU form. By analyzing cases in which the algorithm converges, we obtain a braid classification result, which we also extend to virtual braids, and provide a Mathematica implementation. We discuss other instances of successful "gliding ideas" in the literature – sometimes in disguise – such as the Drinfel'd double construction, Enriquez's work on quantization of Lie bialgebras, and Audoux and Meilhan's classification of welded homotopy links.

Online versions: [BDV].

Keywords: knots, braids, virtual braids, tangles, virtual tangles, diamond lemma, extraction graphs, Drinfel'd double

Mathematics Subject Classification 2020: 57K12, 20F36, 20F38

1. Introduction

In this paper we study *Over then Under* (OU) tangles, a class of oriented tangles in which each strand travels through all of its over-crossings before any of its under-crossings. See Figure 1 for examples; the full definition is given in Section 2.

We present an algorithm (Section 2) which brings non-OU tangle diagrams to OU form using a sequence of *glide moves*: specific isotopies designed to eliminate

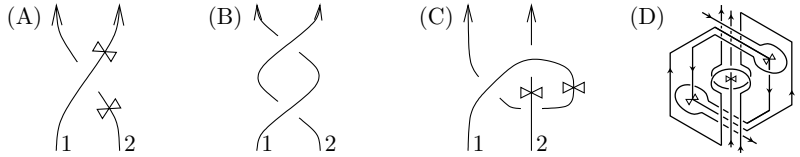

Fig. 1. The tangle diagram (A) is OU as strand 1 is all "over" (so it has an empty "U" part) and strand 2 is all "under" (so it has an empty "O" part). The tangle diagram (B) is not OU: strand 1 is O then U, but strand 2 is U then O. Yet the tangle represented by (B) is OU because it is also represented by (C), which is OU. The diagram (D) is again OU; which familiar tangle does it represent?

any "forbidden sequences" of crossings along a strand. At first glance it seems to converge for any tangle diagram; on closer look, however, one notices that in certain special cases of a strand crossing itself, the glide moves fail.

The goal of this paper is to investigate and review special cases where the gliding algorithm does converge. Indeed, when it does, it can be extremely useful, and in fact gliding ideas have been in use in knot theory and quantum algebra for some time, without being recognised as part of one theme. In our opinion, there is much yet to be gained by looking for further applications; in this paper, we present two applications in detail.

The gliding algorithm converges for braids, and every braid – when considered as a tangle – has a unique OU form. Hence, the OU form is a **separating braid invariant**. We also prove that in fact, tangles which can be brought to OU form are precisely braids, using the identification of the braid group with the mapping class group of a punctured disc (see Section 3).

Even better, the gliding argument extends to virtual braids to show that every virtual braid has a unique OU form when it is regarded as a virtual tangle. With extra work we find that this OU form is a **complete invariant for virtual braids**. This is the subject of Section 4.

Section 5 contains some additional comments, mostly on the relationship between OU tangles and Hopf algebras and on "Extraction Graphs", labeled graphs that are naturally associated with braids and virtual braids by the process of recovering them from their OU forms.

In Section 6 we present Mathematica implementations, including tabulations of virtual pure braids and classical braids.

In Section 7 we review a range of other instances in the literature where "gliding ideas" play a role: the Drinfel'd double construction in quantum groups, a classification of welded homotopy links by Audoux and Meilhan [AM], Enriquez's work on the quantization of Lie bialgebras [En1,En2], and earlier work of the authors.

All tangle diagrams in this paper are *open and oriented*: Their components are always oriented intervals and never circles. For simplicity and definiteness, all tangles in this paper are unframed: we allow all Reidemeister 1 (R1) moves, though

this is not strictly necessary and similar results also hold in the framed case.

2. OU Tangles and Gliding

Definition 2.1. An Over-then-Under (OU) tangle diagram is a tangle whose strands complete all of their over crossings before any of their under crossings, and an OU tangle is an oriented tangle that can be represented by an OU tangle diagram.

This is equivalent to the notion of *ascending* tangles in [ABMW1, Definition 4.15], also called *sorted* in [AM, Definition 1.7] in the context of welded homotopy links.

In greater detail, an OU tangle diagram is an oriented tangle diagram each of whose strands can be divided in two by a "transition point", sometimes indicated with a bow tie symbol $\bowtie$, such that in the first part (before the transition) it is the "over" strand in every crossing it goes through, and in the second part (after the transition) it is the "under" strand in every crossing it goes through, so a journey through each strand looks like an $\mathrm{OO}\ldots\mathrm{O}(\bowtie)\mathrm{UU}\ldots\mathrm{U}$ sequence of crossings. Some examples are shown in Figure 1.

Remark 2.2. Loosely, an OU tangle is the "opposite" of an alternating tangle: crossings along each strand read OOOUUU rather than OUOUOU.

Good mathematics is often discovered via wrong proofs and false theorems, which we mine for the truth still contained within. But in academic writing, one presents only the final product. Here, we take a half-page detour from academic tradition to present a Fheorem (false theorem), which, while it ultimately fails, illustrates the idea and potential of *gliding*. The reader who prefers tradition should rest assured that everything in the paper from Discussion 2.3 onwards is true.

Fheorem 2.1 (Gliding). Every tangle is an OU tangle.

Froof. As in Figure 2, the froof is frivial. Assume first that strands 1 and 2 are already in OU form (meaning, all their O crossings come before all their U ones) but strand 3 still needs fixing, because at some point it goes through two crossings, first under and then over, as on the left of Figure 2. Simply glide strand 1 forward along and over 3 and glide strand 2 back and under 3 as in Figure 2, and the UO interval along 3 is fixed, and nothing is broken on strands 1 and 2 — strand 1 was over and remains over (more precisely, the part of strand 1 that is shown here is the "O" part), and strand 2 is under and remains under.

In fact, it doesn't matter if strands 1 and 2 are already in OU form because as shown in the second part of Figure 2, glide moves can be performed "in bulk". All that the fixing of strand 3 does to strands 1 and 2 is to replace an O by an OOO on strand 1 and a U by a UUU on strand 2, and this does not increase their

complexity as UU...UOO...O sequences can be fixed in one go using bulk glide moves. □

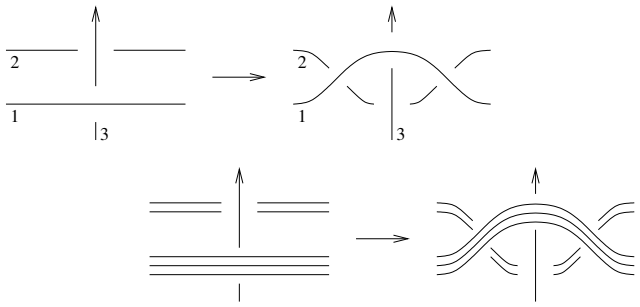

Fig. 2. Glide moves between two crossings and bulk glide moves.

Forollary 2.2. All long knots are trivial.

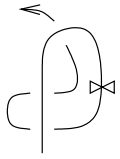

Froof. It is clear that any OU tangle on a single strand is trivial for it must be descending as in the example on the right. □

Discussion 2.3. Forollary 2.2 is clearly false, and so froof of the Gliding Fheorem (2.1) must be false. Indeed, while everything we said about glide moves holds true, there is another way a strand may be U and then O: the U and O may be parts of a single crossing, as on the right, instead of belonging to two distinct crossings, as in the left hand side of the glide move.

It is tempting to dismiss this with "it's only a Reidemeister 1 (R1) issue, so one may glide all kinks to the tail of a strand and count them at the end". Except the same issue can arise in "bulk" UU...UOO...O situations (as now on the right), where it cannot be easily dismissed. One may attempt to resolve the UUOO situation on the right using single (non-bulk) glide moves. We have no theoretical reason to expect this to work as the lengths of UU...U and OO...O sequences may build up faster than they are sorted. And indeed, it doesn't work. Figure 3 shows what happens.

It is true (and also follows from Corollary 3.10) that the only 1-component OU tangle is the trivial one. 2.3

Discussion 2.4. What can we salvage from the disappointing failure of gliding? There are many options to consider. Perhaps Fheorem 2.1 becomes true if we restrict to some subset of the set of all tangles? (Braids, Section 3). Or perhaps if we extend

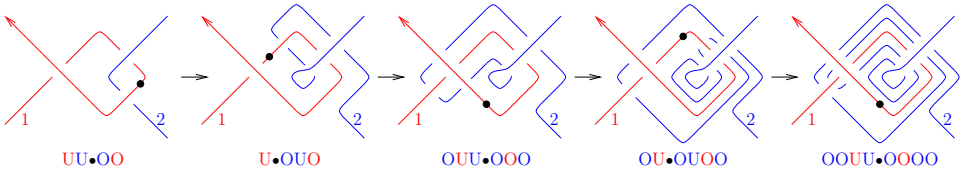

Fig. 3. An attempt to fix a non-OU tangle diagram. In each step we use a single glide move to fix the first UO sequence encountered on strand 1 (we mark it with a •), but things get progressively more complicated. The O/U sequences below the diagrams are listed from the perspective of strand 1.

to some superset? Or in a subset of a superset? (Virtual braids, Section 4). Perhaps we ought to look at some form of finite-type completion? Perhaps we should look at tangles in manifolds? At quotients of the space of tangles? At some combinations of these?

In the authors' opinion it is worthwhile to explore these options. In fact, many of these options have already been explored, each in a different context and without the realization that these different contexts share a common theme: see Section 7. 2.4

3. The Classical Case

We start with a characterization of the tangles for which the gliding procedure of Fheorem (2.1) does in fact work: in Theorem 3.8 we find that these are precisely braids. The following definition gets to the heart of what makes a tangle "problematic" for the gliding procedure:

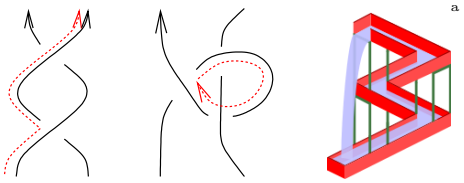

Definition 3.1. Let D be a tangle diagram. A "cascade path" along D is a directed path that travels along strands of D consistently with their orientation, except at crossings where it can (but doesn't have to) drop from the upper strand to the lower strand (but not the other way around). Two examples are on the right. The diagram D is called "acyclic" if it has no "Escher waterfalls" — that is, if no closed cascade paths can be drawn on D. On the right, the first example is acyclic while the second isn't.

[a]Public domain waterfall image from https://commons.wikimedia.org/wiki/File:Waterfall.svg.

Example 3.2. Braid diagrams are acyclic tangle diagrams, and OU tangle diagrams are acyclic tangle diagrams. The stacking product (illustrated on the right) of two acyclic tangle diagrams is again an acyclic tangle diagram.

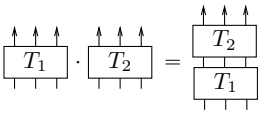

Glide moves and bulk glide moves as in Figure 2 do not change the acyclicity of a tangle diagram. Indeed by simple inspection the possible transits of a cascade path through either of the sides of a glide move are $1 \to 1$, $1 \to 2$, $1 \to 3$, $2 \to 2$, $3 \to 2$, and $3 \to 3$, with numbering as in Figure 2.

Note that if a tangle diagram is OU then no Reidemeister 3 (R3) moves can be performed on it without breaking the OU property — if one side of an R3 move is OU, the other necessarily isn't. This suggests that perhaps an OU form of a tangle diagram is unique up to Reidemeister 2 (R2) moves. We aim to prove this next.

Theorem 3.3. *A tangle diagram D can be made OU using glide moves if and only if it is acyclic, and in that case, the resulting OU tangle diagram, which we call $\Gamma(D)$, is uniquely determined.*

Proof. In an acyclic tangle diagram the U and the O of a UO interval cannot belong to the same crossing (or else an Escher waterfall is present) so the number of UO intervals can be reduced using bulk glide moves as in the Froof of the Gliding Fheorem (2.1). By the observation above, the resulting diagram is still acyclic so the process can be continued.

For the "only if" part, note that OU diagrams are acyclic so anything linked to OU diagrams by glide moves must be acyclic too.

Now to show that $\Gamma(D)$ is unique, observe that when UO intervals are apart from each other, their fixing is clearly independent. It remains to see what happens when UO intervals are adjacent, and there are only two distinct cases to consider. Both of these cases are shown in Figure 4 along with their OU fixes, which are clearly independent of the order in which the glide moves are performed. □

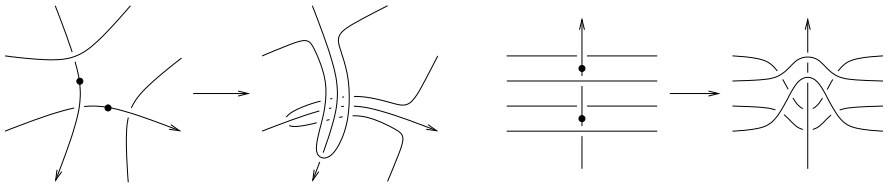

Fig. 4. Two possibilities for "interacting" UO intervals (each marked with a • symbol).

Corollary 3.4. *The stacking product followed by* Γ *makes OU tangle diagrams into a monoid.* □

Definition 3.5. A tangle diagram is called reduced if its crossing number cannot be reduced using only R1 and R2 moves.

Corollary 3.6. *The map* Γ *descends to a well-defined map* $\bar{\Gamma}$ *from "acyclic tangle diagrams modulo Reidemeister moves that preserve the acyclic property" into "reduced OU tangle diagrams".*

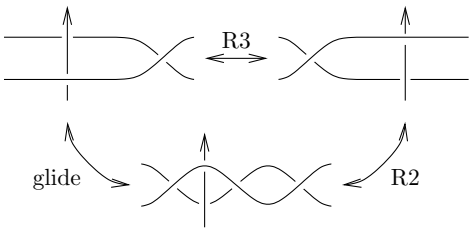

Proof. If two tangle diagrams differ by an R3 move then exactly one of them has a UO interval within the scope of the R3 move, and its elimination via a glide move (which may as well be performed first) yields the other diagram, up to an R2 move (picture on right). Furthermore, R1 and/or R2 moves before a glide become R1 and/or R2 moves after the glide, or they make the glide move redundant, see examples in Figure 5. So the end result of the gliding process of an acyclic tangle is unique modulo R1 and R2 moves. Finally it is easy to check that within any equivalence class of acyclic tangle diagrams modulo R1 and R2 moves that preserve the acyclic property, there is a unique reduced representative. □

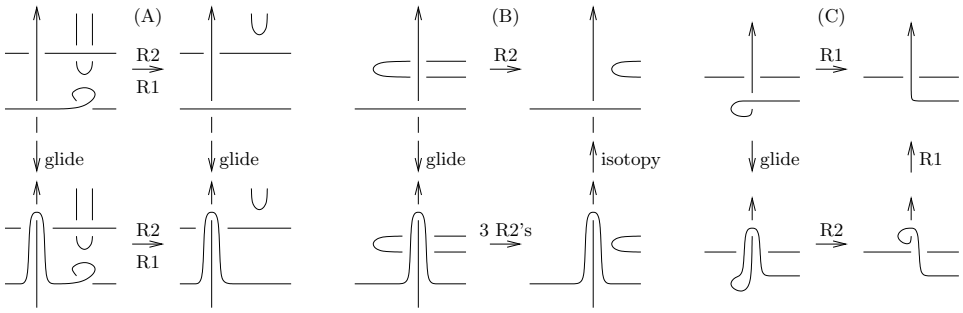

Fig. 5. R1 and R2 moves "commute" with glides (A), or they make glides redundant (B), (C).

Corollary 3.7. *Braids act on reduced OU tangle diagrams both on the left and on the right.*

Proof. Use the stacking product, the fact that braids are always acyclic, and Corollary 3.6. □

In summary, we have a commutative diagram as follows:

$$\begin{array}{ccccc} \mathcal{BD}_n & \xhookrightarrow{\iota} & \mathcal{ACD}_n & \xrightarrow{\Gamma} & \mathcal{OUD}_n \\ \downarrow & & \downarrow & & \downarrow \\ \mathcal{B}_n & \xrightarrow[\text{Theorem 3.8: } \cong]{\bar{\iota}} & \mathcal{AC}_n & \xrightarrow[\cong]{\bar{\Gamma}} & \mathcal{ROU}_n \end{array}$$

Here $\mathcal{BD}_n$ denotes the monoid of braid diagrams with n strands, $\mathcal{ACD}_n$ denotes the monoid of acyclic tangle diagrams with n strands, $\mathcal{OUD}_n$ denotes the monoid of OU tangles diagrams with n strands, ι is the inclusion map, the vertical maps are all "reductions": modulo braid moves in the first column, modulo Reidemeister moves that preserve the acyclic property in the second column, and modulo R1 and R2 in the third column (alternatively, the third vertical map maps OU tangle diagrams to their unique reduced form, and $\mathcal{ROU}_n$ is really a subset of $\mathcal{OU}_n$), and finally, $\bar{\iota}$ is the map induced by ι on the quotient $\mathcal{B}_n$. Note that $\bar{\Gamma}$ is an isomorphism — its inverse is the inclusion $\mathcal{ROU}_n \to \mathcal{AC}_n$ from Example 3.2.

Theorem 3.8 (Classical Isomorphism). *$\bar{\Gamma} \circ \bar{\iota}$ is an isomorphism (and hence also $\bar{\iota}$).*

Proof. Figure 6 contains a visual description of $\bar{\Gamma} \circ \bar{\iota}$. If $\beta \in \mathcal{B}_n$ is a braid, to compute $\bar{\Gamma}(\bar{\iota}(\beta))$ make a whisk in the shape of β from black metal wires, and dip it slightly into a rectangular pool of tahini sauce. Sprinkle lines of green ground parsley on top of the tahini pool, connecting the ends of the whisk to the front side of the pool, as in (A) of Figure 6. The green tahini lines together with the black whisk lines together still make the shape of β, and this will remain true throughout this proof.

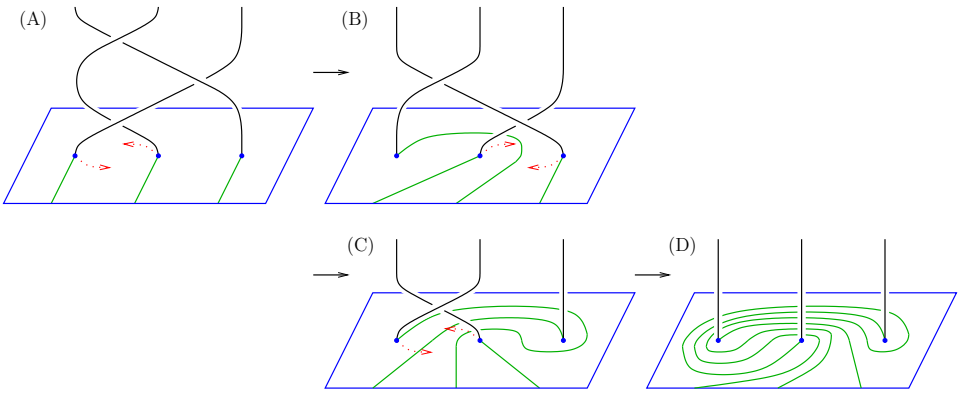

Fig. 6. Stirring a pool of tahini sauce garnished with parsley lines using a braid whisk.

Now slowly push the whisk down and let it stir the sauce as in (B), (C), and

(D) of Figure 6. Less and less of the whisk remains visible and at the same time the green parsley lines remain planar but get more and more twisty. The end of the process is in (D) and it can be interpreted as an OU tangle, by reading the picture from top to bottom: the black whisk wires are all O, and the green parsley lines are all U.[b]

Each step of this stirring process can be broken up into glide moves and planar equivalences that require no Reidemeister moves, as shown in a schematic manner in Figure 7. Hence our process computes $\bar{\Gamma}(\bar{\iota}(\beta))$.

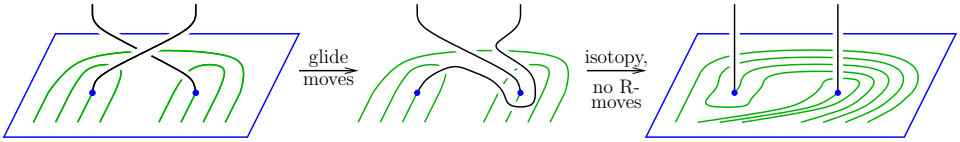

Fig. 7. Stirring is gliding.

Every OU tangle diagram T has a black-green presentation as in (D) of Figure 6. Indeed the O parts of T cannot cross each other so they can be drawn as a collection of straight parallel black lines, and the U parts do cross the O parts so perhaps they cannot be drawn as straight lines, but they still do not cross each other so they make a collection of "green" lines, leading to a picture as in (D) of Figure 6 or as in (A) of Figure 8.

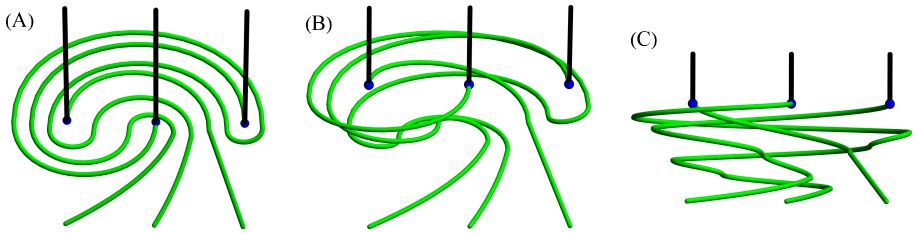

Fig. 8. The map Λ turning an OU tangle into a braid.

Figure 8 also shows how to define a map Λ from OU tangles into braids: draw an OU tangle T as in (A) of Figure 8, and gradually pull down the green strands to below the tahini level by an amount proportional to their arc-length distance from

[b]Readers may recognize this as the identification of the braid group with the mapping class group of a punctured disk. See e.g. [BB, Theorem 1].

their meeting points with the black strands, while at the same time moving your viewpoint to be on the tahini plane, as shown in (B) and (C) of Figure 8. At the end of the process what you see is the braid $\Lambda(T)$.

Both compositions of $\bar{\Gamma} \circ \bar{\iota}$ and of Λ are identity maps[c], and hence $\bar{\Gamma} \circ \bar{\iota}$ is invertible. □

Hence, we have constructed a separating braid invariant:

Corollary 3.9. *$\bar{\Gamma} \circ \bar{\iota}$ is a complete invariant of braids.* □

And in fact, in classical case, OU tangles are merely braids (though we will see in Sections 4 and 7 that there is more to our story):

Corollary 3.10. *All OU tangles are equivalent to braids.* □

Corollary 3.11. *The two actions of Corollary 3.7 of braids on reduced OU diagrams are simple and transitive.* □

4. The Virtual Case

Much is already written about virtual knot theory (see for example [Ka1,Ka2,Ma]) here we give a quick summary of some basic ideas. Classical knots, braids, and tangles can all be defined following the mould "properly annotated planar graphs with univalent and quadrivalent vertices and with properties PPP, modulo local relations RRR". Virtual knots, braids, and tangles are exactly the same, except that the word "planar" is removed from the mould and otherwise nothing is changed. See some examples in Figure 9.

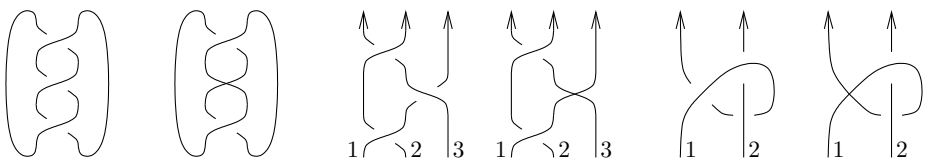

Fig. 9. A 3-crossing knot and a 2-crossing virtual knot, a 3-crossing braid and a 2-crossing virtual braid, and a 3-crossing tangle and a 2-crossing virtual tangle.

[c]Hints: For $\Lambda \circ (\bar{\Gamma} \circ \bar{\iota}) = I_{\mathcal{B}}$ note that the stirring process of Figure 6 can be carried out with the green lines already pulled down as in Figure 8 and when looking from the side, one sees a dance of braid diagrams, which is an equivalence of braids. For $(\bar{\Gamma} \circ \bar{\iota}) \circ \Lambda = I_{\mathcal{ROU}}$ one has to start from a whisk W of the form of (C) of Figure 8 (namely, a whisk that when considered from above, as in (A) of Figure 8, appears to be made of n straight vertical bars and n non-intersecting planar strands). Then one has to show that stirring tahini with parsley lines using W will recreate the shape of W (minus the vertical bars) in the parsley lines.

Note that all the virtual examples in Figure 9 contain a feature like ⤫, often called a "virtual crossing". A "virtual crossing" is **not a crossing**: It is merely an artifact of the fact that when a non-planar graph is drawn on a piece of paper, some edges will intersect, even though from a graph-theoretic perspective these intersections are not vertices, and not part of the data of the graph.

In this paper virtual tangles and virtual braids are always "pure": the ordering of the ends of strands around the boundary of a planar domain has no graph theoretical meaning, for the planar domain itself has no graph theoretic meaning. Yet it makes sense to consider virtual objects whose strands are labelled by some finite set S, and once this is done, virtual tangles become a monoid and virtual braids become a group, where the product[d] of T_1 (or B_1) with T_1 (or B_2) is the disjoint union operation of graphs, followed by the "stitching" of the head of strand a in T_1 (or B_1) to the tail of strand a in T_2 (or B_2), for every $a \in S$.

Thus the virtual (pure) braid group on n strands is the group with generators σ_{ij} "strand i crosses over strand j in a positive crossing" where $i \neq j \in \underline{n}$ and $\underline{n}$ is some fixed set with n elements (perhaps $\underline{n} = \{1, \dots, n\}$), and with relations matching the R3 move and the fact that crossings that involve totally distinct strands commute:

$$v\mathcal{PB}_n = \langle \sigma_{ij} : \ \sigma_{ij}\sigma_{ik}\sigma_{jk} = \sigma_{jk}\sigma_{ik}\sigma_{ij} \text{ and } \sigma_{ij}\sigma_{kl} = \sigma_{kl}\sigma_{ij} \rangle,$$

where it is understood that i, j, k, l are arbitrary distinct elements of $\underline{n}$. For example, the two braids in Figure 9 are $\sigma_{12}\sigma_{31}^{-1}\sigma_{23}$ and $\sigma_{12}\sigma_{23}$ (the first was introduced as a classical braid, but it is also a pure virtual braid).

We let $v\mathcal{PBD}_n$ denote the monoid of all virtual braid diagrams on n strands: namely, the monoid of all words in the generators $\sigma_{ij}^{\pm}$, with no relations.

With this said, everything in Section 3 up to but not including the Classical Isomorphism Theorem (3.8) makes sense and holds true in the virtual case as well, for nothing there depends on the planarity of diagrams. Hence we have a commutative diagram:

$$\begin{array}{ccccc}
v\mathcal{PBD}_n & \xhookrightarrow{\iota_v} & v\mathcal{ACD}_n & \xrightarrow{\Gamma_v} & v\mathcal{OUD}_n \\
\downarrow & & \downarrow & & \downarrow \\
v\mathcal{PB}_n & \xrightarrow{\bar{\iota}_v} & v\mathcal{AC}_n & \xrightarrow[\cong]{\bar{\Gamma}_v} & v\mathcal{ROU}_n \\
 & \searrow^{Ch} & & & \nearrow
\end{array}$$

In this diagram everything was already defined or is the obvious virtual analog of its counterpart in the classical case and does not need a definition, except that we give a special name, the *Chterental map* $Ch := \bar{\Gamma}_v \circ \bar{\iota}_v$, to the composition along the

[d]In the "Geography vs. Identity" language of [BN6], compositions of classical tangles/braids are "Geography", because they are defined using the placements of the ends being stitched, while compositions of virtual tangles/braids are "Identity" because they are defined using the identity of the ends being stitched.

bottom. Yet in contrast with the Classical Isomorphism Theorem (3.8) we have the Theorem 4.1 below. This theorem is originally due to Oleg Chterental [Ch1,Ch2] in a different context; our version is reformulated and independently proven, see a comparison in Discussion 5.1. The proof presented in this section also leads to a new graph-valued braid and virtual braid invariant, see Discussion 5.3 and Section 6.

Theorem 4.1. *([Ch1,Ch2], independent proof below) $Ch = \bar{\Gamma}_v \circ \bar{\iota}_v$, and hence $\bar{\iota}_v$, is injective but not surjective.*

Hence the following corollaries hold true:

Corollary 4.2. *[Ch1,Ch2] Ch is a complete invariant of virtual pure braids.*[e] □

Corollary 4.3. *[Ch1,Ch2] The two actions of virtual pure braids on reduced virtual OU diagrams are simple but not transitive.* □

Corollary 4.4. *[Ch1,Ch2] Not all virtual OU tangles are equivalent to virtual pure braids.* □

Discussion 4.1. The rest of this section is devoted to a proof of Chterental's Theorem (4.1). The idea is to "extract" as much of a virtual braid out of a virtual OU tangle T as possible, by extracting one braid generator at a time while reducing the complexity of what remains of T. The process won't always invert *Ch* (for *Ch* is not invertible), yet it will invert *Ch* on the image of virtual braids, which is enough. The main tools will be the Division Lemma (4.10) which gives a necessary and sufficient condition for the extraction of one braid generator, and the Diamond Lemma (4.12), which will guarantee that this extraction process always terminates with a well-defined answer.

Definition 4.5. If $T \in v\mathcal{AC}_n$ is a virtual acyclic tangle, let $\xi(T)$ denote the crossing number of $\bar{\Gamma}_v(T)$, its R1- and R2-reduced OU form (not counting virtual crossings, of course). We say that a virtual braid $\beta \in v\mathcal{PB}_n$ divides a virtual acyclic tangle $T \in v\mathcal{AC}_n$, and write $\beta \mid T$, if when β is extracted out of T, this reduces the crossing number. In other words, if $\xi(\beta^{-1}T) < \xi(T)$. In that case, we call $\beta^{-1}T$ the quotient of T by β.

Example 4.6. The figure on the right shows two virtual OU tangles, T_1 and T_2. We have that $\sigma_{12} \mid T_1$ and $\sigma_{12}^{-1}T_1 = T_2$. On the other hand, T_2 is not divisible by anything, as it can be readily verified that $\xi(T_2) = 2$ while $\xi(\sigma_{12}^{\pm 1}T_2) > 2$ and $\xi(\sigma_{21}^{\pm 1}T_2) > 2$.

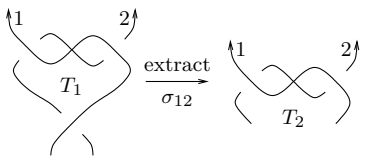

[e]Other separation result for virtual braids are at [GP,BCP].

Example 4.7. The figure on the right shows in its left part the Garside "positive half twist" braid on 3 strands, which happens to be OU in its given presentation, fit within a hexagon summarizing its five divisors σ_{12}, σ_{23}, $\sigma_{12}\sigma_{13}$, $\sigma_{23}\sigma_{13}$, $\sigma_{12}\sigma_{13}\sigma_{23} = \sigma_{23}\sigma_{13}\sigma_{12}$, and the five resulting quotients. This hexagon is also an example of an extraction graph; see Discussion 5.3.

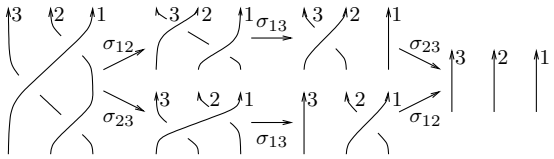

Please bear with us and read the following two examples carefully, as they play a role in the proof of Chterental's Theorem (4.1).

Example 4.8. The k-twist braids are the braids $(\sigma_{12}\sigma_{21})^{k/2}$ (for even k) or $\sigma_{21}(\sigma_{12}\sigma_{21})^{(k-1)/2}$ (for odd k). They are shown along with their reduced OU forms, the Cinnamon Roll tangles CR_k, in Figure 10. Clearly, $\sigma_{21} \mid CR_{2k+1}$ with $\sigma_{21}^{-1} CR_{2k+1} = CR_{2k}$ and $\sigma_{12} \mid CR_{2k}$ with $\sigma_{12}^{-1} CR_{2k} = CR_{2k-1}$, and so we have the following chain of divisibilities and quotients:

$$\cdots \longrightarrow CR_4 \xrightarrow{\sigma_{12}} CR_3 \xrightarrow{\sigma_{21}} CR_2 \xrightarrow{\sigma_{12}} CR_1 \xrightarrow{\sigma_{21}} CR_0. \tag{4.2}$$

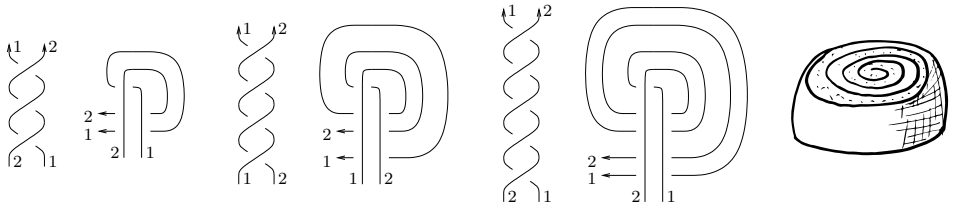

Fig. 10. The 3-twist, 4-twist, and 5-twist braids, and their reduced OU forms the Cinnamon Roll tangles CR_3, CR_4, and CR_5. The equivalence of the twist braids with their respective cinnamon rolls should be clear to anyone who has observed how a kink in a band becomes a twisted band upon tugging. The bonus cinnamon roll was purchased from https://thenounproject.com/.

Example 4.9. A slashed cinnamon roll is a cinnamon roll with an extra always-over strand separating the O-parts of its two curving strands, as shown in (A) of Figure 11. A slashed cinnamon roll is divisible by both σ_{21}^{-1} and σ_{23}, and the quotients, after reductions by many R2 moves, are (B) and (C) of Figure 11. These quotients are themselves cinnamon rolls (with extras on the side), and so they can be divided and reduced further as in Example 4.8, leading to (D) and (E) of Figure 11. Note also that (D) can be reduced to (E) by dividing first by σ_{23} and then by σ_{12}, as shown. Finally, note that we have two paths going from (A) to (E), via (B) and (D) and via (C), and that each defines a braid word by reading the

divisors along it. We claim that these two braid words are equal in $v\mathcal{PB}_3$. Namely, that

$$\sigma_{21}^{-1}\sigma_{13}\sigma_{31}\sigma_{13}\sigma_{31}\sigma_{13}\sigma_{23}\sigma_{21} = \sigma_{23}\sigma_{13}\sigma_{31}\sigma_{13}\sigma_{31}\sigma_{13}. \tag{4.3}$$

Indeed, to see the equality, slide strand 2 across the 5-twist in the following picture[f]:

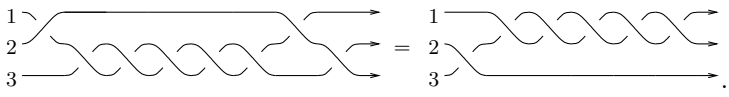

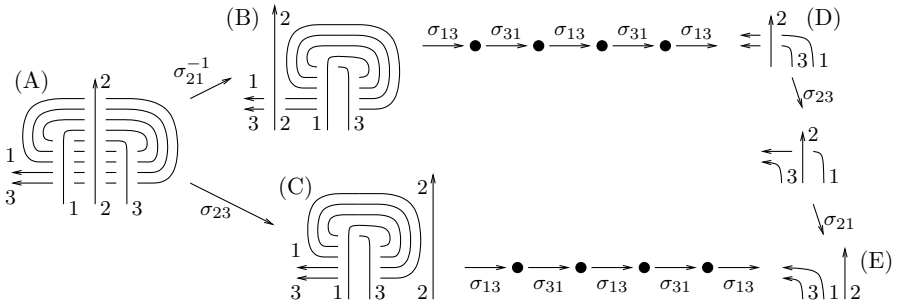

Fig. 11. A slashed cinnamon roll and its quotients down to the identity.

Discussion 4.4. Next, we would like to understand precisely when does a braid generator σ_{ij} divide a reduced virtual OU tangle T, and what is the quotient $\sigma_{ij}^{-1}T$, as a reduced OU tangle. This is done in Figure 12. In (A) of that figure we display σ_{ij}^{-1} at the bottom and T at the top. T could be complicated, but it turns out we only care about what it looks like near the O part of strand j[g]. So in (A) we also display strand i just to remember that it exists, and the O part of strand j, up to its transition point the $\bowtie$. In that part strand j crosses over a number of other strands, or over its own U part, or i's U part, and perhaps with multiplicity. We summarize that by showing only two strands passing under, with no care for their identity or orientation.

In (B) of Figure 12 we attach $\sigma_{ij}^{-1}T$ to T. The result is typically not OU and not reduced. In (C) we glide the part where i goes over j past the $\bowtie$, to make the result OU. We indicate the part of strand i that got moved, from one $\bullet$ to the other, by γ

[f]The equality also follows from Chterental's Theorem (4.1), but we haven't proven Chterental's Theorem yet, and in fact, the proof of Chterental's Theorem depends on the equality.
[g]"Near" in a combinatorial sense, meaning "one or two crossings away from". Not in any metric sense, of course.

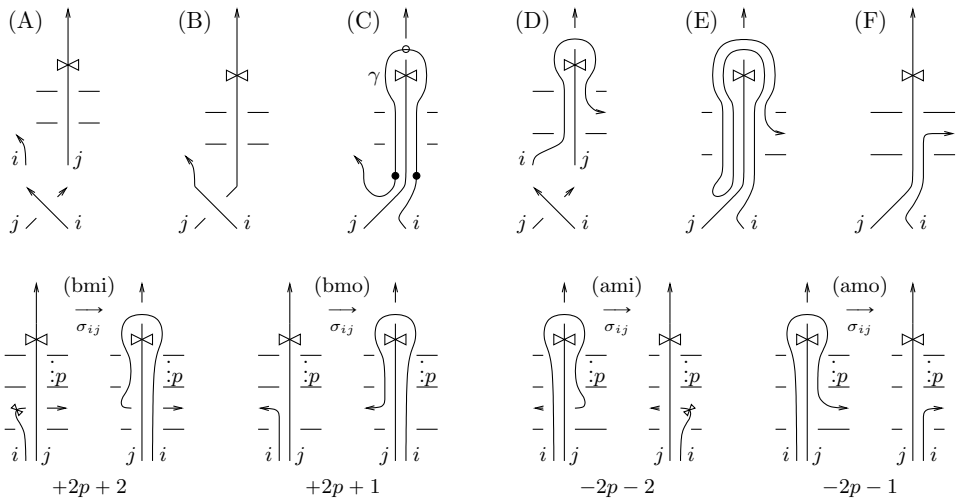

Fig. 12. Everything we need to know about divisibility and quotients.

and note that γ has a natural mid-point, indicated with a $\circ$. Note that the tangle in (C) might not be reduced! That would be the case if as in (D), strand i was to follow γ (backwards) at least a part of the way. For had this been the case, the OU form of $\sigma_{ij}^{-1}T$ would look like in (E), and would be reducible to (F) by R2 moves.

Ergo we care to know precisely how far backwards along γ strand i follows, and when it deviates, precisely how. Four options for the behaviour of i are shown in the lower half of Figure 12: The option "before middle inward", (bmi), means that i traces along γ to before its mid-point, and then deviates by reaching its own transition point $\bowtie$ and turning inwards, to cross under j. In Figure 12 we show both T and the reduced OU form of $\sigma_{ij}^{-1}T$ for option (bmi). If in T there are p further strands passing under j after the deviation point, it is easy to see that $\sigma_{ij}^{-1}T$ gains $2p + 2 > 0$ crossings over T. This is indicated at the bottom of the (bmi) part of Figure 12.

The remaining three options for i are shown in Figure 12 following the same pattern. In option (bmo) strand i deviates from γ before the mid-point and turns outwards, into parts of T we don't display. Here again $\xi(\sigma_{ij}^{-1}T) > \xi(T)$, with a gain of $2p + 1$. In option (ami) strand i follows γ past the mid-point and turns inwards, and in (amo) it turns outwards. In the last two cases $\sigma_{ij}^{-1}T$ loses crossings relative to T, with the precise losses as indicated.

We leave it to the reader to verify that the four options (bmi), (bmo), (ami), and (amo) are mutually exclusive and complete, and that in all cases, if T is reduced to

start with, then $\sigma_{ij}^{-1}T$ as shown in Figure 12 is again reduced[h].

Finally we note that we could repeat the whole discussion for $\sigma_{ij}T$, and everything would be the same, with only a left-right reflection of all the tangles in Figure 12. 4.4

Discussion 4.4 proves the following lemma, which summarizes it:

Lemma 4.10 (Division). *Let $g = \sigma_{ij}^{\pm 1}$ be a generator of $v\mathcal{PB}_n$ and T be a reduced virtual OU tangle.*

(1) $\xi(gT)$ is never equal to $\xi(T)$, so always, either $g^{-1} \mid T$ or $g \mid gT$.
(2) $\sigma_{ij}|T$ if and only if i is parallel[i] to j on its left to its transition point $\bowtie$, and then immediately crosses over j in a positive crossing, as in (ami) and (amo) of Figure 12. Similarly for $\sigma_{ij}^{-1} \mid T$, with "left" replaced with "right" and "positive" with "negative".
(3) If indeed $g \mid T$, the quotient $g^{-1}T$ is determined by how far i pushes backwards on the other side of j, past the point where it crosses over j, and by whether it turns "in" or "out" after that. □

For the continuation of the proof of Chterental's Theorem (4.1) we will need the Diamond Lemma. For completeness we provide a full formulation and a proof. While it is well-known [Be,Sa,Sm], we were not able to find a simple exposition in a language sufficiently similar to ours.

Definition 4.11. A binary relation $\to$ defined on a set $\mathcal{X}$ is called Noetherian if there are no infinite sequences $(x_i) \in \mathcal{X}$ such that $x_1 \to x_2 \to \dots$ (in particular, never $x \to x$, for $x \in \mathcal{X}$). The "transitive closure" of $\to$, denoted $\twoheadrightarrow$, is the binary relation on $\mathcal{X}$ defined by

$$(x \twoheadrightarrow y) \iff (\exists x_0, \dots, x_n \in \mathcal{X} \text{ such that } x = x_0 \to x_1 \to \dots \to x_n = y).$$

[h]In short, if T is reduced and T' is obtained from it by adding and/or removing a number of crossings, when is T' non-reduced? If an R1 or an R2 got added, or if a crossing got added which along with an existing crossing creates an R2, or if crossings are removed between a pair of existing or newly added crossings so as to remove the separation between them and turn them into an R2 pair, or if crossings are removed along a kink to create an R1. One must inspect that none of these possibilities can occur here.

[i]Note that we are in topology / combinatorics, not in geometry, so "i is left-parallel to j" means "anything j does i does in tandem", and not "i and j maintain a constant distance between them". More precisely, "i is left-parallel to j" means "any strand that crosses under j in a positive crossing then crosses under i in a positive crossing (with no other crossings in between), any strand that crosses under j in a negative crossings crossed under i right before in a negative crossing (with no other crossings in between), and i and j encounter those pairs of crossings in the same order".

It is clear that $\twoheadrightarrow$ is transitive and taking $n = 0$ we see that it is reflexive. A non-empty subset $\mathcal{Y}$ of $\mathcal{X}$ is called connected if whenever $y \in \mathcal{Y}$ and $x \in \mathcal{X}$ satisfies $x \to y$ or $y \to x$, then $x \in \mathcal{Y}$. We say that $\to$ satisfies the diamond condition if for every $a, b, c \in \mathcal{X}$ such that $a \to b$ and $a \to c$, there is some $d \in \mathcal{X}$ such that $b \twoheadrightarrow d$ and $c \twoheadrightarrow d$ ("every wedge can be completed to a diamond", as on the right).

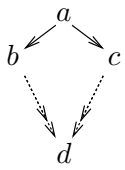

Lemma 4.12. *(The Diamond Lemma, [Ne]) If a Noetherian relation $\to$ on a set $\mathcal{X}$ satisfies the diamond condition then every connected subset $\mathcal{Y} \subset \mathcal{X}$ has a unique final element. Namely, there is a unique $f \in \mathcal{Y}$ such that for every $y \in \mathcal{Y}$, $y \twoheadrightarrow f$.*

Proof. If $t \in \mathcal{Z} \subset \mathcal{X}$, we say that t is $\mathcal{Z}$-terminal if there is no $z \in \mathcal{Z}$ with $t \to z$. By the Noetherian property, every non-empty $\mathcal{Z}$ has a terminal element (perhaps many). Set

$$\mathcal{G} := \{x \in \mathcal{X} : \text{there is a } \textit{unique}\ \mathcal{X}\text{-terminal } \tau(x) \text{ such that } x \twoheadrightarrow \tau(x)\}.$$

Clearly if $x \in \mathcal{G}$ and $x \twoheadrightarrow y$, then $y \in \mathcal{G}$ and $\tau(x) = \tau(y)$ (*). If $\mathcal{B} := \mathcal{X} \backslash \mathcal{G}$ is non-empty, pick some $\mathcal{B}$-terminal element $a \in \mathcal{B}$. If $b, c \in \mathcal{X}$ and $a \to b$ and $a \to c$, find d such that $b \twoheadrightarrow d$ and $c \twoheadrightarrow d$. As a is $\mathcal{B}$-terminal, $b, c, d \in \mathcal{G}$ so by (*) $\tau(b) = \tau(d) = \tau(c)$. Hence all the followers b of a have the same $\tau(b)$, and hence $a \in \mathcal{G}$ with $\tau(a) = \tau(\text{any follower})$ (if a has no followers take $\tau(a) = a$). But this contradicts $a \in \mathcal{B}$, so $\mathcal{B}$ is empty and $\mathcal{G} = \mathcal{X}$.

Now if $x, y \in \mathcal{X}$ and $x \to y$ then $\tau(x) = \tau(y)$, so by connectivity τ is constant on $\mathcal{Y}$. Call that constant f. □

Definition 4.13. Let $\mathcal{X}_n = v\mathcal{PB}_n \times v\mathcal{ROU}_n$. We define a binary relation $\to$ on $\mathcal{X}_n$ as follows

$$\begin{aligned}(\beta_1, T_1) \to (\beta_2, T_2) &\iff \text{for some } g = \sigma_{ij}^{\pm 1} :\ g \mid T_1,\ T_2 = g^{-1} T_1, \text{ and } \beta_2 = \beta_1 g \\ &\iff \text{for some } g = \sigma_{ij}^{\pm 1} :\ \xi(T_2) < \xi(T_1),\ T_2 = g^{-1} T_1, \text{ and } \beta_2 = \beta_1 g.\end{aligned}$$

Example 4.14. With a bit of thought, four examples of elements (A), (B), (C), and (D) of $\mathcal{X}_3$, in fact of $\mathcal{PB}_3 \times \mathcal{ROU}_3$, can be seen in Figure 6. Precisely, the "whisk" part of each of the figures is the braid part β, and the "parsley" part becomes an OU tangle if the whisk is replaced by a straight "identity" whisk as in image (D). These elements are related in the opposite manner to the figure: (D)→(C)→(B)→(A).

Discussion 4.5. Note that if $(\beta_1, T_1) \to (\beta_2, T_2)$ then $\beta_1 T_1 = \beta_2 T_2$ and T_2 is "simpler" than T_1. Thus "flowing with $\to$" agrees with our plan from Discussion 4.1.

Note also that if $(\beta_1, T_1) \to (\beta_2, T_2)$ then β_2 and T_2 are determined by β_1 and T_1 and a single generator g of $v\mathcal{PB}_n$, which we can mark atop the $\to$ symbol as $(\beta_1, T_1) \xrightarrow{g} (\beta_2, T_2)$. With this in mind, a $\twoheadrightarrow$-relation in $\mathcal{X}_n$, meaning a $\to$-chain, is determined by a pair

$$\left(\beta_0,\ T_0 \xrightarrow{g_0} T_1 \xrightarrow{g_1} T_2 \xrightarrow{g_2} \cdots \xrightarrow{g_{m-1}} T_m\right)$$

where β_0 is a virtual braid, and where each g_k is a generator of $v\mathcal{PB}_n$ and for every k, $g_k \mid T_k$ and $T_{k+1} = g_k^{-1} T_k$. The $\to$-chain corresponding to such a pair is

$$(\beta_0, T_0) \xrightarrow{g_0} (\beta_0 g_0, T_1) \xrightarrow{g_1} (\beta_0 g_0 g_1, T_2) \xrightarrow{g_2} \cdots \xrightarrow{g_{m-1}} (\beta_0 \prod g_k, T_m)$$

An example with β_0 suppressed is in Example 4.8. It can be completed by choosing β_0 arbitrarily.

Finally, note that a diamond in $\mathcal{X}_n$ is determined a single virtual braid β_0 and two chains as above with a shared initial tangle,

(4.6)

$$\begin{array}{ccccccccccc} & & T_1 & \xrightarrow{g_1} & T_2 & \xrightarrow{g_2} & \cdots & \xrightarrow{g_{m-2}} & T_{m-1} & & \\ & \overset{g_0}{\nearrow} & & & & & & & & \overset{g_{m-1}}{\searrow} & \\ T_0 = T'_0 & & & & & & & & & & T_m = T'_{m'}, \\ & \underset{g'_0}{\searrow} & & & & & & & & \underset{g'_{m'-1}}{\nearrow} & \\ & & T'_1 & \xrightarrow{g'_1} & T'_2 & \xrightarrow{g'_2} & \cdots & \xrightarrow{g'_{m'-2}} & T'_{m'-1} & & \end{array}$$

with the additional requirement that $\prod g_k = \prod g'_k$ in $v\mathcal{PB}_n$ (which also implies that the chains share their end tangles). An example of such a diamond, with the initial β_0 suppressed, is in Figure 11. 4.5

Lemma 4.15. *The relation $\to$ satisfies the conditions of the Diamond Lemma.*

Proof. As crossing numbers are always finite and $\to$ decreases the crossing number of the tangle part, $\to$ is Noetherian. To verify the diamond condition we must start with a reduced OU tangle $T_0 = T$ and two generators g_0 and g'_0 that divide it, and "complete a diamond" as in Equation (4.6). Let us start with the hardest case.

Case 1. For some i, j, k, $\sigma_{ji}^{-1} \mid T$ and $\sigma_{jk} \mid T$. By (2) of the Division Lemma (4.10), strand j must be left-parallel to strand k to k's $\bowtie$ and right-parallel to strand i to i's $\bowtie$. So the tangle T must contain a part as on the right,

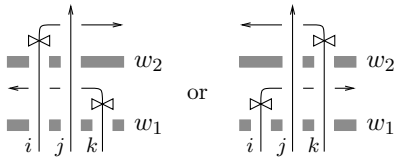

with the two grey bands representing any number w_1 and w_2 of further strands. (Two options for T are shown and we will treat only the first, as the second is mirror image thereof).

In order to complete a diamond, we need to know the quotients $\sigma_{ji} T$ and $\sigma_{jk}^{-1} T$. By (3) of the Division Lemma (4.10), this gets complicated if j continues as a right parallel of k and as a left parallel of i.

Sayeth you: "That's impossible! One can't be to the left of i and also to the right of k!". But unfortunately, it's the topological / combinatorial "left" and "right" that concern us here and the impossible is actually possible. As indicated in Footnote i, "j is right-parallel to k" (to a point) just means that some number $p_k \geqslant 0$ of strands that cross under k then proceed to cross under j, in the same order. As in the figure on the right, this can be drawn while keeping j straight and making the p_k under-strands curve

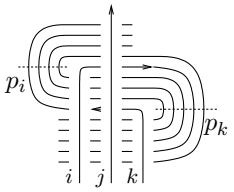

into semi-circles. Similarly, "j is left-parallel to i" (to a point) means, as in the figure, that some number $p_i \geqslant 0$ of arcs cross under both i and j in the manner shown.

Unfortunately, there are many cases to check, depending on the relative sizes of the widths w_1 and w_2, of the "push-back numbers" p_i and p_k, and on whether, at the end, j crosses under i, or under k, or goes elsewhere, as in options (ami) and (amo) of Figure 12. We will try to make it as painless as possible.

The "base cases" occur when

(1) $w_2 = 0$,
(2) $|p_i - p_k| \leqslant 1$,
(3) w_1 is as small as it can be given p_i, p_k, and w_2 (meaning, $w_1 = p_k$ assuming the first two conditions hold).
(4) strand j continues outward relative to both i and k, as in option (amo) of Figure 12.

There are then three possibilities: If $p_k = p_i + 1$, we are looking at a slashed cinnamon roll as in Figure 11, that figure also shows how to complete the diamond, and the required braid relation is Equation (4.3). The cases $p_k = p_i$ and $p_k = p_i - 1$ correspond to slashed cinnamon rolls rolled slightly differently and are shown as (A) and (B) of Figure 13, along with the corresponding diamonds and braids relations. Note that in all of these cases the length of the "twist sequence" $\sigma_{ik}\sigma_{ki}\sigma_{ik}\cdots$ is $p_k + 1$, so these diamonds can be be arbitrarily long.

What if w_1 is bigger than the least it can be given the other parameters (which are otherwise unchanged)? That adds a band of strands at the bottom, as in (A) of Figure 14. This band gets added in the same way everywhere else in Figures 11 and 13, with no change to the resulting diamonds.

What if $p_i > p_k + 1$ (yet respecting the other constraints)? This adds and extra band of strands as in (B) of Figure 14. These bands get tugged along through the processes of Figure 13 with no changes to the end results. A similar thing happens if $p_k > p_i + 1$.

What if $w_2 > 0$ and $p_1 = p_k$ are multiples of $w_2 + 1$? Then we are in (C) of Figure 14, and the slashed cinnamon roll has a band of width w_2 of extra filling! One may check that the extra filling unwinds along with the rest as in Figure 13 with no change to the diamonds. There are similar "filled" versions of the other base cases.

What if $w_2 > 0$ and $p_1 = p_k$ are not round multiples of $w_2 + 1$? Then we are in a situation like (D), which is a combination of previous cases, and the same conclusions apply.

What if we are in an (ami) case instead of (amo)? We are in a situation like in (E), and the same comments apply as for (C). We made j dotted in (E), to make the similarity with (C) easier to see.

What if several of the what ifs are combined? Then some combination of (A)-

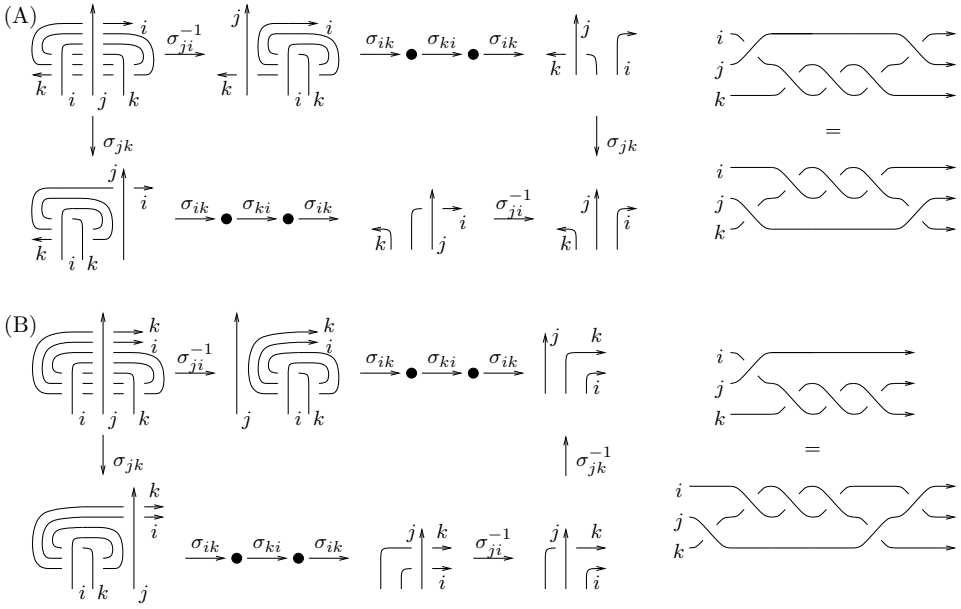

Fig. 13. Two other slashed cinnamon rolls.

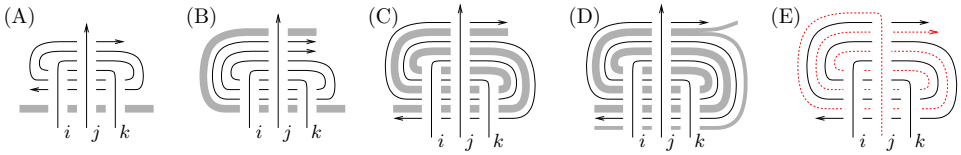

Fig. 14. The what ifs.

(E) of Figure 14 applies, and we leave it to the reader to verify that in all cases, diamonds complete as in Figures 11 and 13.

Case 2. For some i, j, k, $\sigma_{ij} \mid T$ and $\sigma_{jk} \mid T$. By (2) of the Division Lemma (4.10), strand i must be a left-parallel of j and then cross over it, and j must be a left-parallel of k and then cross over it, as shown in Figure 15, along with the completion of the wedge into a diamond. In that figure we took option (amo) for both divisibilities. Option (ami) is possible only for the $\sigma_{ij} \mid T$ divisibility, and makes little difference to the resulting diamond.

Case 3. For some i, j, k, $\sigma_{ij}^{-1} \mid T$ and $\sigma_{jk}^{-1} \mid T$. That's the same as Case 2, with left interchanged with right.

Case 4. For some distinct i, j, k, l, $\sigma_{ij}^{s_1} \mid T$ and $\sigma_{kl}^{s_2} \mid T$, where $s_1, s_2 \in \{\pm 1\}$. In this

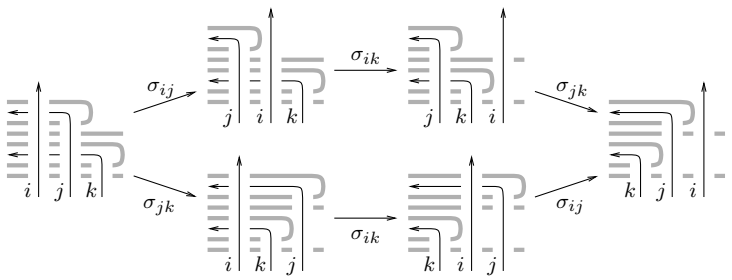

Fig. 15. Case 2 and the resulting diamond.

case division by $\sigma_{ij}^{s_1}$ commutes with division by $\sigma_{kl}^{s_2}$, and the resulting diamond is a square, as in Figure 16.

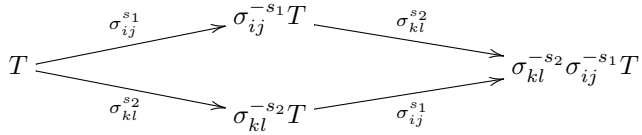

Fig. 16. The diamond for case 4.

There are no further cases to check. If two generators divide T, they involve at most 4 strands, and if they involve exactly 4 strands, that's Case 4. The Division Lemma (4.10) excludes the possibility that the two generators involve only two strands — namely, that they are two of $\{\sigma_{ij}^{\pm 1}, \sigma_{ji}^{\pm 1}\}$. It also excludes the remaining 3-strand cases: namely, that they are $\{\sigma_{ij}, \sigma_{ik}\}$, $\{\sigma_{ik}, \sigma_{jk}\}$, $\{\sigma_{ij}^{-1}, \sigma_{ik}^{-1}\}$, $\{\sigma_{ik}^{-1}, \sigma_{jk}^{-1}\}$, $\{\sigma_{ij}, \sigma_{jk}^{-1}\}$, $\{\sigma_{ij}^{-1}, \sigma_{jk}\}$, or $\{\sigma_{ij}, \sigma_{kj}^{-1}\}$. Each of these exclusions requires a short argument, and we provide only the argument for the first one. Indeed if both $\sigma_{ij} \mid T$ and $\sigma_{ik} \mid T$, then by the Division Lemma strand i is a left parallel of both the O part of j (call it O_j) and the O part of k (call it O_k), showing that at least one of O_j and O_k is empty. Without loss of generality, it is O_j. But then the i over j crossing that the Division Lemma guarantees is the first crossing on both i and j, leaving no room for O_k to be a right parallel of a part of i, unless O_k is also empty. But then the first crossing on i is both over j and over k, which is impossible. □

Proof of Chterental's Theorem (4.1). We have shown that $\mathcal{X}_n = v\mathcal{PB}_n \times v\mathcal{ROU}_n$ with the relation $\to$ satisfies the conditions of the Diamond Lemma. Let $f\colon \mathcal{X}_n \to \mathcal{X}_n$ be the function guaranteed by the Diamond Lemma, mapping every element to the unique final element in its connected component.

Let I denote both the the 0-crossing pure virtual braid on n strands (the identity

element of $v\mathcal{PB}_n$) and the 0-crossing OU tangle on n strands. By (1) of the Division Lemma (4.10), if $\beta', \beta'' \in v\mathcal{PB}_n$ are virtual braids and $g = \sigma_{ij}^{\pm 1}$ is a generator of $v\mathcal{PB}_n$ then

$$\begin{aligned} \text{either} \quad & (\beta' g, Ch(\beta'')) \to (\beta', g\,Ch(\beta'')) = (\beta', Ch(g\beta'')) && \text{if } g^{-1} \mid Ch(\beta'') \\ \text{or} \quad & (\beta', Ch(g\beta'')) = (\beta', g\,Ch(\beta'')) \to (\beta' g, Ch(\beta'')) && \text{if } g \mid g\,Ch(\beta''), \end{aligned}$$

and so by induction on the length of a presentation of $\beta \in v\mathcal{PB}_n$, (β, I) and $(I, Ch(\beta))$ are in the same connected component of $\mathcal{X}_n$. Hence $f(I, Ch(\beta)) = f(\beta, I) = (\beta, I)$, by the Diamond Lemma and as $\xi(I) = 0$ implies that (β, I) is final.

Now if $Ch(\beta_1) = Ch(\beta_2)$ then

$$(\beta_1, I) = f(\beta_1, I) = f(I, Ch(\beta_1)) = f(I, Ch(\beta_2)) = f(\beta_2, I) = (\beta_2, I),$$

so $\beta_1 = \beta_2$, proving the injectivity of Ch.

Note also that we learned that for every $\beta \in v\mathcal{PB}_n$, $(I, Ch(\beta)) \twoheadrightarrow (\beta, I)$, and in particular, $Ch(\beta)$ must be divisible by at least one generator of $v\mathcal{PB}_n$. But Example 4.6 exhibits a virtual OU tangle T_2 that is not divisible by any generator, and hence Ch is not surjective. □

5. Assorted Comments

Discussion 5.1. Virtual OU tangles are equivalent to Chterental's "Virtual Curve Diagrams" (VCDs) [Ch1,Ch2], though we hope that they are a bit more natural, and that they tell a bigger story. We explain the relationship in Figure 17, albeit without repeating Chterental's definitions. Given a virtual curve diagram as in (A) of Figure 17, connect all the curve ends on the upper (dashed) line to the vertical infinity using O curves (thus making everything else into U curves), delete the upper and the lower lines, and get a virtual OU tangle (B). It is positioned opposite to our habits[j] so in order to feel a bit better, we flip the picture over in (C).

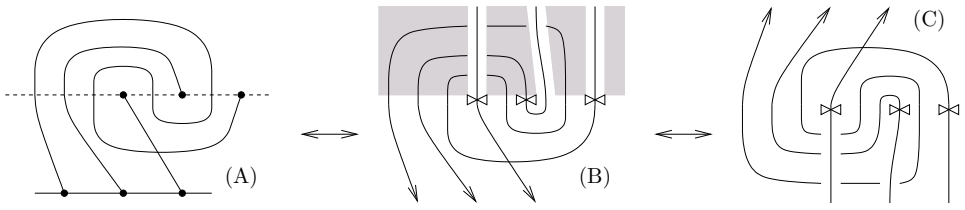

Fig. 17. A Chterental Virtual Curve Diagram (VCD) and the corresponding virtual OU tangle.

[j] We are in topology / combinatorics; these habits are anyway meaningless.

To go back, draw a virtual OU tangle with the O parts of its strands straight, parallel, of equal length, and heading downward (that's always possible as they never cross each other), and then draw the U parts curving between them, perhaps with virtual crossings[k]. Push all the virtual crossings to below the areas between the O strand-parts (in light grey in (B) of Figure 17), re-insert an upper line and a lower line, and get back to (A) of Figure 17, a VCD.

While in a different context, our proof of Chterental's Theorem (4.1) is similar in spirit to Chterental's proof that VCDs can be used to separate virtual braids. A notable difference is that we fully analyze the possible diamonds, instead of relying on the classical Artin's theorem. Another minor difference is that we deal only with pure virtual braids (minor because separating braids that induce different permutations is a non-issue). 5.1

Remark 5.1. The Division Lemma (4.10) implies that if T is classical (namely, is given with a planar presentation in a disk D) and $\sigma_{ij}^{s} \mid T$ with $s \in \{\pm 1\}$, then the beginning points of strands i and j must be adjacent within the boundary of D (with i left of j if $s = +1$ and i right of j if $s = -1$), and then $\sigma_{ij}^{-s}T$ is classical again. By induction, if a virtual braid β divides a classical T, then β is actually classical.

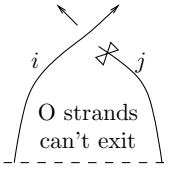

Remark 5.2. Everything within the proof of Chterental's Theorem (4.1) can be restricted to the classical case, hence reproving (in a complicated and very algebraic manner) that the map $\bar{\Gamma} \circ \bar{\iota}$ of the Classical Isomorphism Theorem (3.8) is injective. To show by algebraic means that $\bar{\Gamma} \circ \bar{\iota}$ is also surjective it is enough to show that every non-trivial classical OU tangle T is divisible by at least one $\sigma_{ij}^{\pm 1}$ — dividing and repeating until the process terminates (it must, as crossing numbers decrease), and using the previous remark would show that T is equivalent to a classical braid. The required "existence of a divisor" property is proven as follows: For any strand j let i be the first strand to cross over j after j's transition point $\bowtie$. If the starting points of i and j are adjacent then either σ_{ij} or σ_{ij}^{-1} divides T. Otherwise a "triangular tent shield" is created as on the right, and the same argument can be repeated within it. When the process terminates, we have a divisor. The topological arguments of the classical braids Section (3) are of course a lot simpler.

Remark 5.3. Let $\mathcal{T}_n$ denote the set of all classical tangles with n open strands and let $v\mathcal{T}_n$ denote the set of all virtual tangles with n open strands. We wish to briefly

[k]We've emphasized that "virtual crossings" are **not crossings**. But here we must link with other people's conventions.

study the following two commutative squares, the "classical" and the "virtual":

$$\begin{array}{ccc} \mathcal{B}_n & \xrightarrow{\chi} & \mathcal{T}_n \\ {\scriptstyle \bar{\iota}}\downarrow{\scriptstyle \cong} & \text{1-1} & \uparrow{\scriptstyle \varphi}\text{1-1} \\ \mathcal{AC}_n & \xrightarrow[\cong]{\bar{\Gamma}} & \mathcal{ROU}_n \end{array} \qquad \begin{array}{ccc} v\mathcal{PB}_n & \xrightarrow{\chi_v} & v\mathcal{T}_n \\ {\scriptstyle \bar{\iota}_v}\downarrow\text{1-1} & \text{1-1?} & \uparrow{\scriptstyle \varphi_v}\text{1-1?} \\ v\mathcal{AC}_n & \xrightarrow[\cong]{\bar{\Gamma}_v} & v\mathcal{ROU}_n \end{array}$$

In these squares, $\bar{\iota}$, $\bar{\Gamma}$, $\bar{\iota}_v$, and $\bar{\Gamma}_v$ along with the properties ($\cong$, $\cong$, 1-1, and $\cong$) were discussed in Sections 3 and 4. Also, χ (χ_v) and φ (φ_v) are the obvious maps of (virtual) braids and reduced (virtual) OU tangles into (virtual) tangles[l]. We note that the injectivity of χ was known already to Artin [Ar, Theorem 12][m], and thus it follows that φ is also injective. We do not know if χ_v and φ_v are injective. The injectivity of χ_v was stated as an open problem in [ABMW2, Question 5.1]. Given the injectivity of $\bar{\iota}_v$, the injectivity of χ_v would clearly follow from the injectivity of φ_v, which we conjecture holds true. 5.3

Conjecture 5.1. **The obvious map φ_v of reduced virtual OU tangles into virtual tangles is injective.**

The reason we believe this conjecture is that we see a plausible path to proving it. One way to go would be to find enough invariants of virtual tangles to separate reduced virtual OU tangles. There are plenty of invariants of virtual tangles coming from Hopf algebras and quantum groups, reduced virtual OU tangles are easy to enumerate (they are "free" objects, subject to no relations), and there are precedents where using quantum groups one can find enough invariants to separate near-free objects: for example, quantum $gl(N)$ invariants separate braids [BN1], and braid groups are semi-direct products of free groups.

Discussion 5.2. In fact, there is a very close relationship between virtual OU tangles and Hopf algebras. Denote by $v\mathcal{OU}_q^p$ the set of OU tangles that have p O-only strands and q U-only strands (it is a subset of $v\mathcal{OU}_{p+q}$). We claim that $v\mathcal{OU}_q^p$ is precisely the set of "universal formulas" for linear maps $\mathrm{Hom}(H^{\otimes p} \to H^{\otimes q})$, where H is an arbitrary involutive[n] Hopf algebra[o]: Meaning, those formulas that can be written as an arbitrary composition of the structure maps m, Δ, S, ϵ, and η of H, and that make sense even if H is infinite dimensional (so they contain no cycles).

By means of an example and with all details suppressed, Figure 18 demonstrates how a virtual O/U tangle becomes a Gauss diagram and then a universal Hopf formula. Furthermore, one may show that the relation between the product m and the

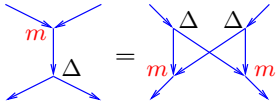

[l]In the vaguest way, χ and φ are pictograms for braids and OU tangles, respectively.
[m]Quick proof: The fundamental group of the complement of a braid along with the n bottom meridians and the n top meridians determines the braid, and this invariant extends to tangles.
[n]Meaning that the antipode S satisfies $S^2 = I$.
[o]Or even, an involutive Hopf object in a symmetric monoidal category.

coproduct Δ in a Hopf algebra (illustrated on the right) can be used to bring all coproducts in a universal Hopf formula to before all the products, and hence every universal Hopf formula comes from an O/U tangle as in Figure 18. 5.2

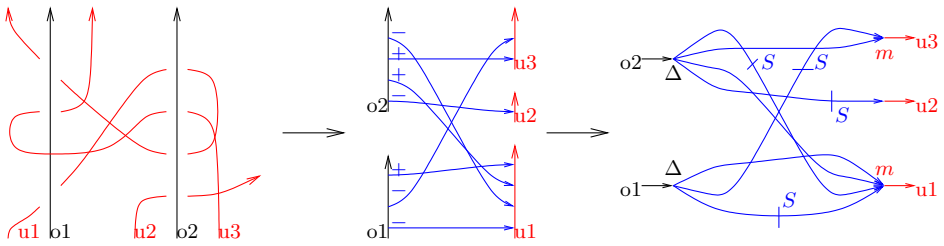

Fig. 18. A virtual O/U tangle in $v\mathcal{OU}_3^2$ becomes a Gauss diagram becomes a universal Hopf formula representing an element of $\mathrm{Hom}(H^{\otimes 2} \to H^{\otimes 3})$. Note that the antipode S is inserted on the $(-)$-marked edges of the Gauss diagram, which correspond to the negative crossings of the tangle.

Remark 5.4. The awkwardness of having to restrict to involutive Hopf algebras suggests that there may be an alternative way to tell the story of this paper that does not require involutivity. Perhaps using "rotational virtual tangles" [Ka2].

Remark 5.5. The map $Ch\colon v\mathcal{PB}_n \to v\mathcal{ROU}_n$ along with Discussion 5.2 imply that there is an invariant of virtual braids with values in $\mathrm{End}(H^{\otimes n})$, where H is an involutive Hopf algebra. Other such invariants exist [Wor,MV]. We expect that they are closely related.

Remark 5.6. It follows from the reasonings of Section 4 that it is possible to extract a maximal braid out of an OU tangle, leaving behind a minimal "core" tangle. Precisely, if a virtual OU tangle T is decomposed as $T = \beta' T'$ where β' is a virtual pure braid and T' is a virtual OU tangle, and if T' has the minimal possible crossing number for such a decomposition, then β' and T' are uniquely detemined. Indeed, let $(\beta', T') = f(I, T)$ be the final element guaranteed by the Diamond Lemma (4.12) in the connected component of (I, T) in $\mathcal{X}$. For example, if T is T_1 of Example 4.6, then $\beta' = \sigma_{12}$ and T' is T_2 of 4.6.

We do not know if the same is true for arbitrary virtual and/or classical tangles. 5.6

Discussion 5.3. There is a lovely visual side to the tools developed for the proof of Chterental's Theorem (4.1). Given a reduced virtual OU tangle $T \in v\mathcal{ROU}_n$, we can consider the part $EG(T)$ of $\mathcal{X}_n$ that lies "below" (I, T):

$$EG(T) := \left\{(\beta', T')\colon\ (I, T) \twoheadrightarrow (\beta', T')\right\}.$$

We restrict the relation $\to$ to $EG(T)$, making it into a directed graph that we name "the extraction graph of T". By first computing $\bar{\Gamma} \circ \bar{\iota}$ or $Ch = \bar{\Gamma}_v \circ \bar{\iota}_v$, we can also define $EG(\beta)$ when β is a braid or a virtual braid. These graphs are in themselves invariants (defined on $v\mathcal{OU}_n$ or $v\mathcal{PB}_n$ or $\mathcal{B}_n$). They are often visually pleasing: we have already seen a few examples, in Examples 4.6 and 4.7, within Equation 4.2, and in Figure 13[p]. Another example, the extraction graph of the classical braid $\sigma_{21}^{-1}\sigma_{13}\sigma_{32}^{-1}\sigma_{21}$ whose closure is the figure-8 knot, is here on the right (we label edges by the relevant divisor $\sigma_{ij}^{\pm 1}$ and vertices by the value of ξ). Some even nicer examples appear in Section 6.4.

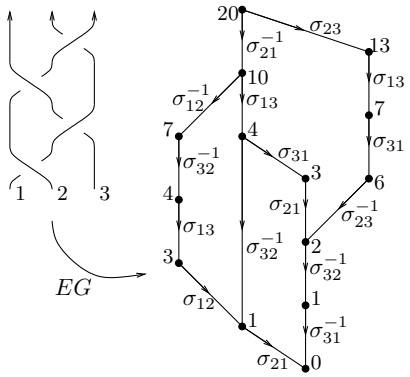

For any T, $EG(T)$ is a finite graph (for the set of potential divisors $\{\sigma_{ij}^{\pm 1}\}$ is finite and and only finitely many divisions can be carried out before we run out of crossings). $EG(T)$ always has an "initial" vertex i (the pair (I, T)) and a final vertex f — the final element that is guaranteed by the Diamond Lemma and that is discussed in Remark 5.6. Every vertex v of $EG(T)$ is sandwiched between the two: $i \twoheadrightarrow v \twoheadrightarrow f$. Every "wedge" in $EG(T)$ (Definition 4.11) can be completed to a diamond of one of the types appearing in Figures 11, 13, 15, and 16 (hence all cycles in $EG(T)$ are of even length, and hence $EG(T)$ is bipartite). If one travels from i to f along any path in $EG(T)$ while reading the generators indicated on the edges, one always reads the same virtual braid.

If T is $\bar{\Gamma}(\iota(\beta))$ or $Ch(\beta)$, the final vertex f of $EG(\beta)$ is (β, I), and every path from i to f spells a braid word for β. Thus $EG(\beta)$ highlights a finite set of "special" braid words for β. It follows from Remark 5.1 that if β is classical then all the special words for it are classical too.

We don't really understand $EG(\beta)$ — we don't know what properties of β can be read off $EG(\beta)$, and we don't know how to characterize the "special words" for β that appear in $EG(\beta)$ other than by repeating the definitions. 5.3

6. Some Computations

When mathematics is computable, we feel it is appropriate and necessary to include an implementation. In this case, the implementation is concise and follows the notation and logical structure of a paper, so we choose to include it as an integral part of that paper. We hope that the programs presented here serve as an illustration of the overall simplicity and validity of the ideas within the paper, and that they

[p]Figure 11 is not example because it misses a part of the graph. See Section 6.4.

encourage others to play and further discover. The implementations also lead to new enumerations – the tables in Sections 6.2 and 6.3 – and to intriguing and appealing graph-valued invariants – Section 6.4 – which cannot be computed otherwise, and which may lead to further study.

All code here is written in *Mathematica* [Wol] and is available as the *Mathematica* notebook *SomeComputations.nb* at [BDV].

6.1. *Implementing virtual OU tangles, virtual braids, and Ch*

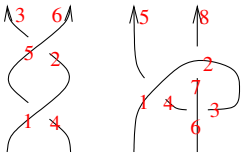

To represent a virtual tangle diagram D on the computer, we order its strands and traverse each of them in order, marking each "O" point, each "U" point, and each end of strand, with the integers $1, 2, 3, \ldots$, in the order in which they are encountered. See examples on the right. For each crossing x of D we form a *Mathematica* expression $\mathtt{X}_s[i, j]$, where s is the sign of the crossing and i and j are the markings next to the O side and the U side of x, respectively. We also form an expression $\mathtt{EOS}[k]$ for each end-of-strand marked k. We toss all this information into a container `VD`, and the result is our computer representation of D. Below, `vd1` and `vd2` are the results of this process for the two example tangles shown here.

```
SetAttributes[VD, Orderless]
```

```
vd1 = VD[X+1[1, 4], X+1[5, 2], EOS[3], EOS[6]];
vd2 = VD[X+1[1, 4], X+1[2, 7], X+1[6, 3], EOS[5], EOS[8]];
```

Sometimes in a `VD` we allow to label O/U/`EOS` points by arbitrary real numbers, for in fact, only the ordering of these points matter. The routine `Tidy` takes a real-ordered `VD` and converts it to a sequentially ordered one. Thus it brings a `VD` to a "canonical form":

```
Tidy[vd_VD] := Module[{ps = Union @@ (List @@@ vd)},
  Replace[vd, Thread[ps → Range@Length@ps], {2}] ]
```

```
VD[X+1[0.9, 4.2], X+1[5, e], EOS[π], EOS[60]] // Tidy
```

```
VD[EOS[4], EOS[6], X1[1, 2], X1[3, 5]]
```

The routine `R12Reduce1` reduces a virtual diagram by performing one R2 or R1 move, if such a move is available, and otherwise it does nothing. The routine `R12Reduce` finds the fixed point of `R12Reduce1` — in other words, it reduces a virtual diagram using all available R1 and R2 moves.

```
R12Reduce1[vd_VD] := Tidy@Module[{R2s, R2}, Which[
     Length[R2s = Cases[vd, X_s_[i_, j_] :> X_-s[i + 1, j + 1]] ⋂ (List @@ vd)] >
      0,
     Complement[vd, VD[R2 = First@R2s,
       R2 /. X_s_[i_, j_] :> X_-s[i - 1, j - 1]]],
     Length[R2s = Cases[vd, X_s_[i_, j_] :> X_-s[i + 1, j - 1]] ⋂ (List @@ vd)] >
      0,
     Complement[vd, VD[R2 = First@R2s,
       R2 /. X_s_[i_, j_] :> X_-s[i - 1, j + 1]]],
     True, DeleteCases[vd, X_[i_, j_] /; Abs[i - j] == 1] ]];
R12Reduce[vd_VD] := FixedPoint[R12Reduce1, vd]
```

Here's a very minor example:

```
VD[X_+1[1, 4], X_-1[2, 5], EOS[3], EOS[6]] // R12Reduce
```

```
VD[EOS[1], EOS[2]]
```

In a similar manner, $\Gamma 1$ performs one glide move if one is available, and $\bar{\Gamma}$ fully reduces under both glide moves and R1 and R2 moves. Here we bound the number of iterations by 2^{24}, to artificially stop runaway reductions such as the one in Figure 3.

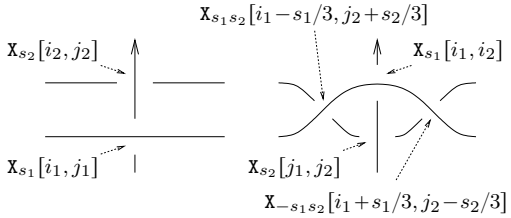


```
Γ1[vd_VD] := Module[{js, s1, i1, j1, s2, i2, j2},
  js = Cases[vd, X_[_, j_] :> j] ⋂ Cases[vd, X_[i_, _] :> i - 1];
  If[Length[js] == 0, vd,
   j1 = RandomChoice[js]; i2 = j1 + 1;
   Cases[vd, X_s_[i_, j1] :> (s1 = s; i1 = i)];
   Cases[vd, X_s_[i2, j_] :> (s2 = s; j2 = j)];
   Tidy@Join[Complement[vd, VD[X_s1[i1, j1], X_s2[i2, j2]]],
     VD[X_s2[j1, j2], X_s1[i1, i2], X_s1 s2[i1 - s1 / 3, j2 + s2 / 3],
      X_-s1 s2[i1 + s1 / 3, j2 - s2 / 3]]
    ] ]]
```

```
Γ̄[vd_VD] := FixedPoint[Γ1@*R12Reduce, vd, 2^24];
Γ̄[T_] /; Head[T] =!= VD := Γ̄[VD[T]]
```

As expected, $\bar{\Gamma}(\texttt{vd1}) = \texttt{vd2}$:

```
Γ̄[vd1] == vd2
```

```
True
```

Next we define the composition operation `d1**d2` of virtual tangle diagrams. The implementation works by "shrinking" `d2` so that each of its strands would fit between the last crossing in the corresponding strand of `d1` and the `EOS` at the end of that strand of `d1`, then taking the union of `d1` and the shrank `d2`, and then applying `Tidy` to the result:

```
VD /: d1_VD ** d2_VD := Tidy@Module[{es1, es2, m2},
   es1 = Cases[d1, EOS[i_] :> i];
   m2 = Max[es2 = Cases[d2, EOS[i_] :> i]];
   d1 ⋃ Replace[DeleteCases[d2, _EOS],
     i_ :> i / m2 - 1 + es1[[1 + Count[es2, e_ /; i > e]]], {2}]]
```

For example, "our" `vd2` has 3 crossings yet is equivalent to a 2-twist braid. So `vd1 · vd2` ought to have 6 crossings while its reduced OU form, $\bar{\Gamma}$(`vd1 · vd2`) should be the Cinnamon Roll CR_4, which has 7 crossings. The computer agrees:

```
{vd2 ** vd2, Γ̄[vd2 ** vd2]}
```

```
{VD[EOS[9], EOS[14], X₁[1, 4], X₁[2, 11], X₁[5, 8],
  X₁[6, 13], X₁[10, 3], X₁[12, 7]], VD[EOS[9], EOS[16], X₁[1, 8],
  X₁[2, 15], X₁[3, 6], X₁[4, 13], X₁[10, 7], X₁[11, 14], X₁[12, 5]]}
```

Next we implement virtual pure braids, and it is best to start with an example. We represent the 3-strand virtual pure braid $\beta = \sigma_{21}^{-1}\sigma_{13}\sigma_{31}\sigma_{13}\sigma_{31}\sigma_{13}\sigma_{23}\sigma_{21}$ of Example 4.9 by the *Mathematica* expression below:

```
β = VPB[3, σ̄₂,₁, σ₁,₃, σ₃,₁, σ₁,₃, σ₃,₁, σ₁,₃, σ₂,₃, σ₂,₁];
```

The conversion of `VPB`s into `VD`s is quite easy. We just need to define it on the generators and then use the already-available composition of `VD`s to extend the definition to products of generators:

```
VPB[n_] // VD := VD @@ (EOS /@ Range[n]);
VPB[n_, σ_i_,j_] // VD :=
 Tidy@Append[VD @@ (EOS /@ Range[n]), X₊₁[i - 0.5, j - 0.5]];
VPB[n_, σ̄_i_,j_] // VD :=
  Tidy@Append[VD @@ (EOS /@ Range[n]), X₋₁[i - 0.5, j - 0.5]];
VPB[n_, σ_, σs__] // VD := VD[VPB[n, σ]] ** VD[VPB[n, σs]]
```

We can compute $Ch(\beta) = \bar{\Gamma}_v(\bar{\iota}_v(\beta))$ (count that it has 18 `X` symbols, just as Figure 11 (A) has 18 crossings!):

```
β // VD // Γ̄
```

```
VD[EOS[14], EOS[24], EOS[39], X_1[20, 6], X_1[21, 31],
 X_1[22, 10], X_1[23, 35], X_1[1, 38], X_1[2, 13], X_1[3, 34],
 X_1[4, 9], X_1[5, 30], X_1[15, 37], X_1[16, 12], X_1[17, 33], X_1[18, 8],
 X_1[19, 29], X_1[25, 36], X_1[26, 11], X_1[27, 32], X_1[28, 7]]
```

We can even verify Equation (4.3):

```
(β // VD // Γ̄) == (VPB[3, σ2,3, σ1,3, σ3,1, σ1,3, σ3,1, σ1,3] // VD // Γ̄)
```

```
True
```

6.2. *Tabulating Virtual Pure Braids*

Our next task is to tabulate virtual pure braids with a given number of strands n and a bound m on the number of crossings. The first routine, `VPBGens`, outputs the list of all generators of $v\mathcal{PB}_n$:

```
A_ \ B_ := Complement[A, B];
VPBGens[n_] :=
  VPBGens[n] = Flatten@Table[{σi,j, σ̄i,j}, {i, n}, {j, Range[n] \ {i}}];
```

```
VPBGens[3]
```

```
{σ1,2, σ̄1,2, σ1,3, σ̄1,3, σ2,1, σ̄2,1, σ2,3, σ̄2,3, σ3,1, σ̄3,1, σ3,2, σ̄3,2}
```

Next we'd like to generate all words in the generators we just computed, and separate them using *Ch* and Chterental's Theorem (4.1). To save some computer effort, we generate only "proud" words — words that do not contain a letter followed by its inverse, or adjacent commuting letters that are not in lexicographic order. The "Proud Followers" `PF` of a generator are those generators that can follow it without ruining the pride of a word:

```
PF[n_, σi_,j_] := PF[n, σi,j] = Module[{p, q, s},
    Flatten@{σi,j, σj,i, σ̄j,i,
      Table[{σp,q, σq,p, σ̄p,q, σ̄q,p}, {p, {i, j}}, {q, Range[n] \ {i, j}}],
      Table[{σp,q, σ̄p,q}, {p, Range[i + 1, n] \ {j}},
       {q, Range[n] \ {i, j, p}}] }];
PF[n_, σ̄i_,j_] := PF[n, σ̄i,j] = PF[n, σi,j] /. σi,j → σ̄i,j
```

```
PF[4, σ2,3]
```

```
{σ2,3, σ3,2, σ̄3,2, σ2,1, σ1,2, σ̄2,1, σ̄1,2, σ2,4, σ4,2, σ̄2,4,
 σ̄4,2, σ3,1, σ1,3, σ̄3,1, σ̄1,3, σ3,4, σ4,3, σ̄3,4, σ̄4,3, σ4,1, σ̄4,1}
```

And then `PVPBDs`$[n, m]$ computes all Proud Virtual Pure Braid Diagrams on n strands and with m crossings:

```
PVPBDs[n_, 0] := {VPB[n]};
PVPBDs[n_, 1] := VPB[n, #] & /@ VPBGens[n];
PVPBDs[n_, m_] :=
 Flatten[PVPBDs[n, m - 1] /.
   VPB[n, σs___, σ_] :> (VPB[n, σs, σ, #] & /@ PF[n, σ])]
```

```
PVPBDs[2, 2]
```

$$\{\mathrm{VPB}[2, \sigma_{1,2}, \sigma_{1,2}], \mathrm{VPB}[2, \sigma_{1,2}, \sigma_{2,1}], \mathrm{VPB}[2, \sigma_{1,2}, \overline{\sigma}_{2,1}], \mathrm{VPB}[2, \overline{\sigma}_{1,2}, \overline{\sigma}_{1,2}],$$
$$\mathrm{VPB}[2, \overline{\sigma}_{1,2}, \sigma_{2,1}], \mathrm{VPB}[2, \overline{\sigma}_{1,2}, \overline{\sigma}_{2,1}], \mathrm{VPB}[2, \sigma_{2,1}, \sigma_{2,1}], \mathrm{VPB}[2, \sigma_{2,1}, \sigma_{1,2}],$$
$$\mathrm{VPB}[2, \sigma_{2,1}, \overline{\sigma}_{1,2}], \mathrm{VPB}[2, \overline{\sigma}_{2,1}, \overline{\sigma}_{2,1}], \mathrm{VPB}[2, \overline{\sigma}_{2,1}, \sigma_{1,2}], \mathrm{VPB}[2, \overline{\sigma}_{2,1}, \overline{\sigma}_{1,2}]\}$$

These sets grow very rapidly:

```
PVPBDs[4, 4] // Length
```

```
219 560
```

`AllVPBs`$[n, m]$ finds representatives for all virtual braids on n strands with at most m crossings, by using `PVPBDs`$[n, m]$ and then deleting duplicates by $\bar{\Gamma}_v$:

```
AllVPBs[n_, m_] :=
 DeleteDuplicatesBy[Γ̄]@Flatten@Table[b, {k, 0, m}, {b, PVPBDs[n, k]}]
```

```
AllVPBs[2, 2]
```

$$\{\mathrm{VPB}[2], \mathrm{VPB}[2, \sigma_{1,2}], \mathrm{VPB}[2, \overline{\sigma}_{1,2}], \mathrm{VPB}[2, \sigma_{2,1}], \mathrm{VPB}[2, \overline{\sigma}_{2,1}],$$
$$\mathrm{VPB}[2, \sigma_{1,2}, \sigma_{1,2}], \mathrm{VPB}[2, \sigma_{1,2}, \sigma_{2,1}], \mathrm{VPB}[2, \sigma_{1,2}, \overline{\sigma}_{2,1}], \mathrm{VPB}[2, \overline{\sigma}_{1,2}, \overline{\sigma}_{1,2}],$$
$$\mathrm{VPB}[2, \overline{\sigma}_{1,2}, \sigma_{2,1}], \mathrm{VPB}[2, \overline{\sigma}_{1,2}, \overline{\sigma}_{2,1}], \mathrm{VPB}[2, \sigma_{2,1}, \sigma_{2,1}], \mathrm{VPB}[2, \sigma_{2,1}, \sigma_{1,2}],$$
$$\mathrm{VPB}[2, \sigma_{2,1}, \overline{\sigma}_{1,2}], \mathrm{VPB}[2, \overline{\sigma}_{2,1}, \overline{\sigma}_{2,1}], \mathrm{VPB}[2, \overline{\sigma}_{2,1}, \sigma_{1,2}], \mathrm{VPB}[2, \overline{\sigma}_{2,1}, \overline{\sigma}_{1,2}]\}$$

There are 15,156 virtual pure braids with 3 strands and precisely 4 crossings (meaning, braids in `AllVPBs`$[3, 4]$ but excluding those in `AllVPBs`$[3, 3]$). It took our computer about 86 seconds to figure that out:

```
Length@AllVPBs[3, 4] - Length@AllVPBs[3, 3] // Timing
```

```
{85.9844, 15 156}
```

$m\backslash n$	2	3	4	5	6
0	1	1	1	1	1
1	4	12	24	40	60
2	12	132	504	1,320	2,820
3	36	1,416	10,344	41,760	124,140
4	108	15,156	211,416	1,308,360	5,357,700
5	324	162,156	4,317,912		
6	972	1,734,864			

In our spare time we have tabulated the numbers of n-strand pure virtual braids with precisely m crossings for some small values of n and m. The results are on the right, and data files containing the actual braids are at [BDV]. As a test of the integrity of our programs we also computed most of the numbers in this table by generating all braid words and reducing modulo all relations[q]. The numbers match. See the *Mathematica* notebook *VPBByGensAndRels.nb* at [BDV].

6.3. *Tabulating Classical Braids*

It is a bit odd that we have not seen a table such as the one above, but for classical braids. As the classical braid group is automatic [Ep] and hence the word problem in it is very easy, there are much better in-theory tools than ours to produce such a table. Yet our tools are implemented in practice, and we may as well use them.

First, we need to be able to convert from a standard classical braid notation [BM] to the VPB notation used here.

```
VPB[BR[n_, is_List]] :=
  VPB[n, Module[{π = Range@n, i}, Sequence @@ Table[
      If[i > 0,
       π⟦{i, i + 1}⟧ = π⟦{i + 1, i}⟧; σ_{π⟦i+1⟧,π⟦i⟧},
       (* else *) π⟦{-i, -i + 1}⟧ = π⟦{-i + 1, -i}⟧; σ̄_{π⟦-i⟧,π⟦-i+1⟧} ],
      {i, is}] ]];
VD[br_BR] := VD[VPB@br]
```

```
BR[3, {1, 2, 1}] // VPB
```

```
VPB[3, σ_{1,2}, σ_{1,3}, σ_{2,3}]
```

After that, we repeat the same steps as in the virtual case:

```
PF[n_, i_Integer] :=
  (Range[Max[Abs[i] - 1, 1], n - 1] ⋃ (-Range[Max[Abs[i] - 1, 1], n - 1])) \
   {-i};
```

[q]Sometimes two braid words of length m_1 are related by a chain of relations that pass through words of length m_2, where $m_2 > m_1$, and we do not know in advance a bound on m_2. Hence the computation using generators and relations is slow (as we have to raise m_2 and the number of words to consider grows very big) and unreliable (strictly speaking, we only get upper bounds on the braid counts).

```
PF[7, -4]
```

```
{-6, -5, -4, -3, 3, 5, 6}
```

```
ProudBs[n_, 0] := {BR[n, {}]};
ProudBs[n_, 1] := BR[n, {#}] & /@ (Range[n - 1] ⋃ (-Range[n - 1]));
ProudBs[n_, m_] /; m > 1 :=
 Flatten[ProudBs[n, m - 1] /.
   BR[n, {σs___, σ_}] :> (BR[n, {σs, σ, #}] & /@ PF[n, σ])]
```

```
AllBs[n_, m_] := DeleteDuplicatesBy[Reverse]@
  Flatten@Table[b, {k, 0, m}, {b, ProudBs[n, k]}]
```

For example, here are all the distinct positive 3-strand braids:

```
PositiveQ[BR[_, σs_]] := And @@ (# > 0 & /@ σs);
Select[AllBs[3, 3], PositiveQ]
```

```
{BR[3, {}], BR[3, {1}], BR[3, {2}], BR[3, {1, 1}],
 BR[3, {1, 2}], BR[3, {2, 1}], BR[3, {2, 2}], BR[3, {1, 1, 1}],
 BR[3, {1, 1, 2}], BR[3, {1, 2, 1}], BR[3, {1, 2, 2}],
 BR[3, {2, 1, 1}], BR[3, {2, 2, 1}], BR[3, {2, 2, 2}]}
```

On our computer, it takes about 20 seconds to find that there are 1,110 classical braids with 4 strands and crossing number equal to 5:

```
Length@AllBs[4, 5] - Length@AllBs[4, 4] // Timing
```

```
{20.1875, 1110}
```

And here's a table of the numbers of n-strand pure virtual braids with precisely m crossings, for small values of n and m. The data files containing the actual braids are at [BDV].

$m\backslash n$	2	3	4	5	6
0	1	1	1	1	1
1	2	4	6	8	10
2	2	12	26	44	66
3	2	30	98	206	362
4	2	68	338	884	1,794
5	2	148	1,110	3,600	8,370
6	2	314	3,542	14,198	37,606
7	2	656	11,098	54,876	164,910
8	2	1,356	34,362	209,348	711,746
9	2	2,782	105,546	791,798	3,039,546

Note that the entries in the $n = 3$ column of this table fit with the sequence $6 \cdot 2^m - 2F_{m+3} - 2$, where F_m is the mth Fibonacci number:

```
Table[
 6 × 2^m - 2 Fibonacci[m + 3] - 2,
 {m, 15}]
```

```
{4, 12, 30, 68, 148, 314, 656, 1356,
 2782, 5676, 11532, 23354, 47176, 95108, 191438}
```

The fit persists at least up to $m = 12$. We do not know why this is so.

6.4. *Extraction Graphs*

We can now write a short program `EG`, to compute and display Extraction Graphs as in Discussion 5.3.

```
Options[EG] = {Labels → False, GraphLayout → "SpringElectricalEmbedding",
   EdgeStyle → Automatic};
```

```
EG[∅_, opts___] :=
 Module[{vd, n, gs, vs, es = {}, e, p = 0, m1, m2, g, q, k, lbl},
  lbl = Labels /. {opts} /. Options[EG];
  gs = VPBGens[n = Count[vd = Γ̄[∅], _EOS]]; vs = {vd};
  While[p < Length[vs], m1 = Count[vd = vs[[++p]], X_[_, _]];
   Do[m2 = Count[q = Γ̄[VD[VPB[n, g /. {σ → σ̄, σ̄ → σ}]] ** vd], X_[_, _]];
    If[m2 < m1, If[! MemberQ[vs, q], AppendTo[vs, q]];
     e = p ↔ Position[vs, q][[1, 1]];
     AppendTo[es, If[lbl, Labeled[e, g], e] ] ],
    {g, gs}] ];
  Graph[Table[If[lbl, Labeled[k, Length[vs[[k]]] - n], k], {k, p}], es,
   FilterRules[Join[{opts}, Options[EG]], Options[Graph]]] ]
```

Note that the diamond in Figure 11 is genuine, but it is not an extraction graph, because the full extraction graph of the initial OU tangle of that figure contains two further edges:

```
EG[VPB[3, σ2,3, σ1,3, σ3,1, σ1,3, σ3,1, σ1,3], Labels → True,
 GraphLayout → {"LayeredDigraphEmbedding", "Orientation" → Left}]
```

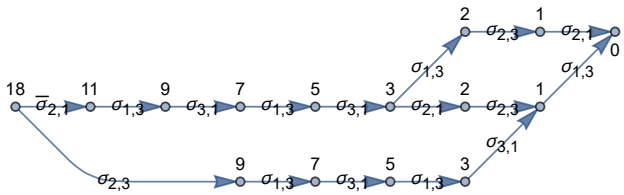

The braid below, suggested to us by B. Wiest, has a linear extraction graph and hence a unique "special word" (see Discussion 5.3), but that word is of length 13, whereas the braid can be presented by a shorter word β, of length 11:

```
β = BR[4, {-2, -3, -2, 1, -2, 1, -2, 1, 3, -2, 1}];
{g = EG[β, Labels → True, GraphLayout → Automatic, ImageSize → Large],
 VertexCount@g - 1, Length@β[[2]]}
```

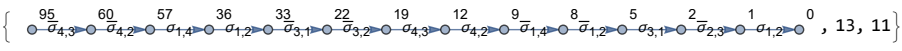

It is easy to see that the extraction graph of the 4-crossing 8-strand braid $\nearrow\nearrow\nearrow\nearrow$ is the tesseract:

```
EG[BR[8, {1, 3, 5, 7}], GraphLayout → "HighDimensionalEmbedding",
  ImageSize → Small]
```

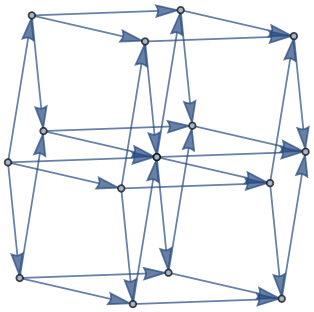

The extraction graphs of Garside braids seem to be permutahedra (we did not attempt to prove this in general):

```
EG[BR[4, {1, 2, 3, 1, 2, 1}], Labels → True]
```

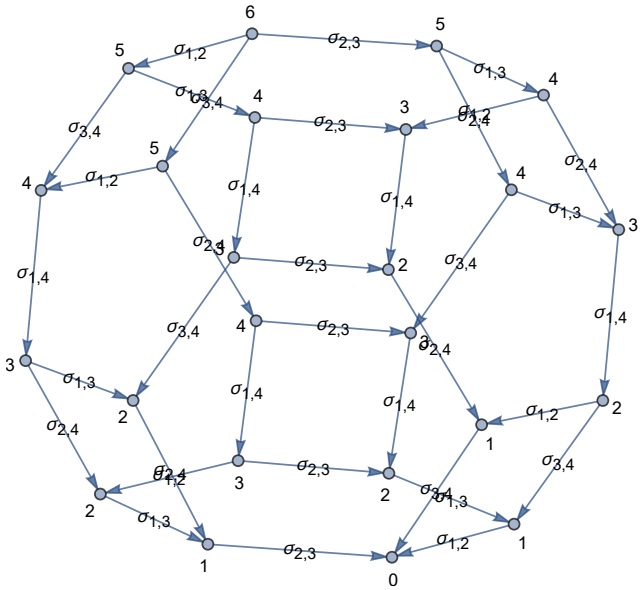


```
EG[BR[5, {1, 2, 3, 4, 1, 2, 3, 1, 2, 1}]]
```

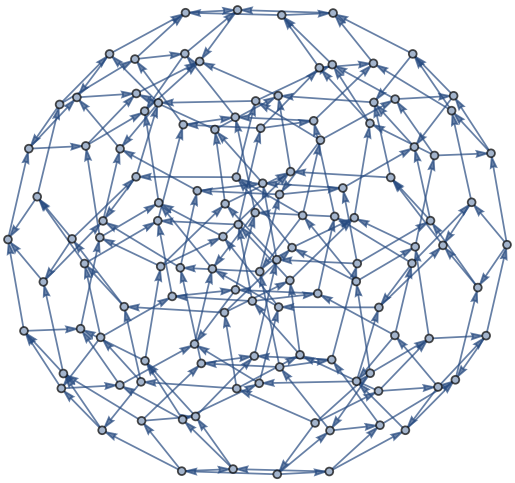

Sometimes extraction graphs can be amusing. In no particular order, here are a lifesaver, an impressionistic map of the US state of Iowa, a torch flame, a legless bird, a feather, a ladder, a tennis racket, and a mouse trap:

```
SetOptions[EG, EdgeStyle → Thick];

g1 = EG[BR[9, {2, -1, -1, -1, 4, 6, 8}]] (* lifesaver *);
g2 = EG[β2 = BR[5, {3, -4, -3, 4, -1, 4, -1, 4, 3, 4, -2, 1}]] (* Iowa *);
g3 = EG[β2, GraphLayout → Automatic] (* torch flame *);
g4 = EG[VPB[6, σ̄6,2, σ2,4, σ4,3, σ̄1,4, σ3,1, σ4,5, σ3,2, σ̄5,2, σ̄3,2, σ̄6,2]]
 (* bird *);

(* feather, ladder, tennis racket, mouse trap *)
g5 = EG[VPB[6, σ5,2, σ2,5, σ5,6, σ5,4, σ̄4,3, σ1,3, σ̄4,6, σ4,2, σ̄4,6, σ4,3,
    σ̄6,1, σ̄5,3, σ2,6, σ4,5, σ4,3, σ̄2,5], GraphLayout → Automatic];
g6 = EG[BR[3, {1, 2, 1, 2, 1, 2, 1, 2, 1, 2, 1, 2, 1, 2, 1, 2}],
   GraphLayout → Automatic];
g7 = EG[BR[3, {2, -1, -1, -1, -1, -1, -1, 2, 1, 1, 2, 2, 1, -2, 1, 1, 2, 1}]];
g8 =
  EG[BR[3, {2, -1, -1, -1, -1, -1, -1, -1, 2, -1, -1, -1, -1, -1,
     -1, -1, -1}]];

ImageCollage[(Scaled[1] → Show[#]) & /@ {g1, g2, g3, g4, g5, g6, g7, g8},
 ImagePadding → 10, Background → White]
```

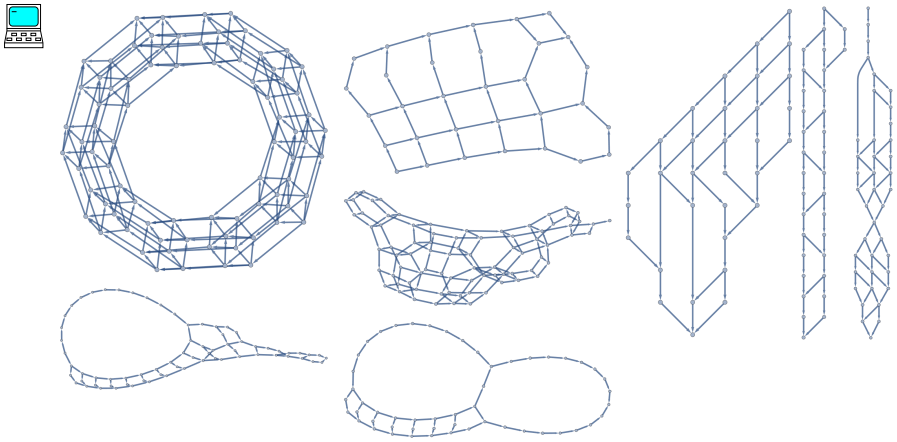

We don't know what, if any, can be learned about braids from these graphs, and we can only hope the referee will forgive us for having a bit of fun.

6.5. *Computational Complexity*

Looking again at Figure 12 (C), we see that in the worst case, if the crossing number $\xi(T)$ of an OU tangle T is p, the crossing number of the OU version of $\sigma_{ij}^{\pm 1}T$ might be as big as $3p+1$, and hence the complexity of computing Ch grows exponentially. Here are the "worst" classical and virtual braids with 8 crossings. A bit more is in the *Mathematica* notebook *TheWorstBraids.nb* at [BDV].

```
Length@Γ̄@BR[3, {-1, 2, -1, 2, -1, 2, -1, 2}] - 3
```

```
172
```

```
Length@Γ̄@VPB[2, σ1,2, σ̄2,1, σ1,2, σ̄2,1, σ1,2, σ̄2,1, σ1,2, σ̄2,1] - 2
```

```
984
```

7. There's more!

There's more! In fact, OU tangles and OU ideas seem prevalent in knot theory, even though it seems that nobody collected all these ideas together before. In fact, possibly the most important contribution of this paper is the observation that, in addition to the detailed examples that we studied throughout, everything mentioned in this section is OU-related.

7.1. *Weakening the Bond*

The Gliding Fheorem (2.1) fails because the bond between the strands of a single crossing is too strong; they cannot be separated to be taken for rides along other

strands in an independent manner: when the U and the O of a UO interval belong to the same crossing, one cannot glide them independently of each other and across each other as the glide move of Figure 2 dictates. So we seek to weaken this bond.

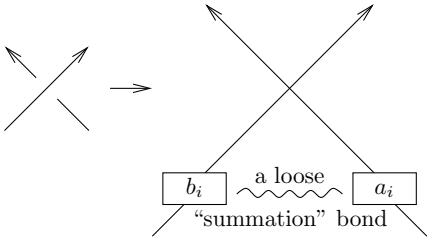

One way to do so is with algebra. One aims to construct invariants of tangles by placing "R-matrices" on positive crossings (and their inverses on negative crossings). An R-matrix is an element $R = \sum_i b_i \otimes a_i \in H \otimes H$ in the tensor square of some algebra H, and its b_i side is placed on the O side of the crossing while its a_i side is put on the U side. This done, one multiplies the algebra elements seen on each strand in the order in which they appear along it, and the hope is that the result would be an invariant of the tangle, living in $H^{\otimes S}$ where S is the set of strands.

In this context "O" becomes "b_i" and "U" becomes "a_i", and the bond between O and U is nearly severed — within a long product, given the appropriate commutation relations, b_i's can be commuted against a_i's whether or not they originally came from the same crossing. Further effort is needed in order to make use of this fact, and it is beyond the scope of this summary to reproduce this effort here. Yet the result becomes "something from nothing": given relatively little input, a construction of an R-matrix and the algebra H in which it lives. This construction is better known as "the Drinfel'd double construction". See more at [BN5] and hopefully in a future publication.

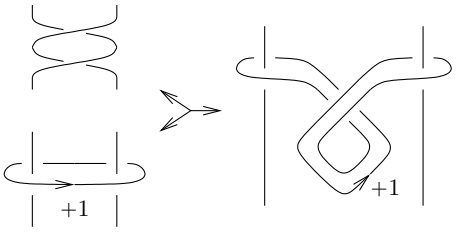

Another way to weaken the bond between the O side and the U side of a single crossing is to represent crossings using surgery. A quick summary is on the right: a crossing can be created using a +1 surgery on a loop surrounding the two strands to be crossed, and that loop is relatively loose bond between these two strands, for in itself it can be pushed around.

This story is imprecise and incomplete: Imprecise because strictly speaking, the surgery shown created two crossings and not just one. Incomplete in several ways; the most important is that general surgeries can change the ambient space from S^3 into another 3-manifold, and thus to properly pursue this idea one must study an appropriate class of tangles in manifolds. See more at [Th] and hopefully in a future publication.

7.2. *Prior Art*

Milnor attempted to classify links up to link homotopy by introducing the "reduced peripheral system" [Mi]. Unfortunately, this is only a complete invariant of

homotopy links with up to three components. In [AM] Audoux and Meilhan use a gliding-type algorithm and OU links to give a full analysis of the kernel of this invariant: namely, they prove that the reduced peripheral system is a complete invariant of *welded* homotopy links (welded links up to *self-virtualization* equivalence). Welded links are closely related to knotted ribbon tori in $\mathbb{R}^4$, and homotopy links map non-injectively into welded homotopy links by "spinning around a plane." See [AM, Definition 1.7], where OU links are called *sorted*. See also [ABMW1, Definition 4.15] where they are called "ascending".

An earlier occurrence of OU ideas in the context of w-tangles is in the paper [BN4] whose theme is the separation of hoops, that can only go Under, from balloons, that go both Under and Over (so [BN4] is a bit less "pure", as the balloons are not quite O). Later within the same paper, and also within [BD2,BD3,BN7], the associated graded space of the space of w-tangles is studied, the space $\mathcal{A}^w$ of "arrow diagrams modulo the TC relation". Furthermore that space is studied using various "Heads then Tails" techniques, which in the language of the current paper, correspond to UO presentations (not OU, but of course, it's essentially the same). See especially [BN7, Section 2.4].

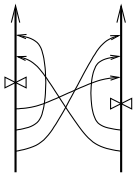

An even earlier occurrence of OU ideas, in the associated graded $\mathcal{A}^v$ context for virtual tangles, occurs in a very well-hidden way within Enriquez' work on quantization of Lie bialgebras [En1,En2]. For example, his "universal algebras" [En2, Section 1.3.2] are isomorphic to the space $\mathcal{A}^v_{OU}$ of arrow diagrams as on the right, in which all arrow tails occur before all arrow heads (that's OU!), and is endowed with the product that $\mathcal{A}^v_{OU}$ inherits from the stacking product of $\mathcal{A}^v$ (which is the analogue of the product used in our paper). We are afraid that there aren't excellent introductions available on $\mathcal{A}^v$ and its relationship with virtual tangles. Hopefully we will write one one day. Until then, some information is in [BD2] and in lecture series such as [BN2,BN3]. We also hope to one day explain the Enriquez work as the construction of a "homomorphic expansion" [BD1] for the space of virtual OU / acyclic tangles.

If $\mathfrak{g} = \mathfrak{a}^\star \bowtie \mathfrak{a}$ is the double of a Lie bialgebra $\mathfrak{a}$, there is a standard interpretation of $\mathcal{A}^v$ as a space of formulas for elements in tensor powers $\mathcal{U}(\mathfrak{g})^{\otimes n}$ of the universal enveloping algebra $\mathcal{U}(\mathfrak{g})$ of $\mathfrak{g}$. Within this context, arrow tails (or "O") correspond to $\mathfrak{a}^\star$ and arrow heads (or "U") correspond to $\mathfrak{a}$, and the O then U theme of this paper corresponds to the "polarization" isomorphism $\mathcal{U}(\mathfrak{g}) \cong \mathcal{U}(\mathfrak{a}^\star) \otimes \mathcal{U}(\mathfrak{a})$, which is a consequence of the PBW theorem. In itself, the polarization isomorphism is central to all approaches to the quantization of Lie bialgebras [EK,Se].

8. Acknowledgement

We wish to thank P. Bellingeri, A. Referees, D. Thurston, and B. Wiest for comments and suggestions, and especially O. Chterental for spotting a major gap in an

earlier version of this paper. This work was partially supported by NSERC grant RGPIN-2018-04350, by the University of Sydney Visiting Scholar Scheme, and by the Chu Family Foundation (NYC).

References

[Ar] E. Artin, *Theory of Braids,* Ann. of Math. **48-1** (1947) 101–126. See pp. 24.

[ABMW1] B. Audoux, P. Bellingeri, J-B. Meilhan, and E. Wagner, *Homotopy Classification of Ribbon Tubes and Welded String Links,* Ann. Sc. Norm. Super. Pisa Cl. Sci. **17-1** (2017) 713–761, arXiv:1407.0184. See pp. 3, 39.

[ABMW2] B. Audoux, P. Bellingeri, J-B. Meilhan, and E. Wagner, *On Usual, Virtual, and Welded Knotted Objects up to Homotopy,* J. Math. Soc. Japan **69-3** (2017) 1079–1097, arXiv:1507.00202. See pp. 24.

[AM] B. Audoux and J-B. Meilhan, *Characterization of the Reduced Peripheral System of Links,* arXiv:1904.04763. See pp. 2, 3, 39.

[BN1] D. Bar-Natan, *Vassiliev and Quantum Invariants of Braids,* in Proc. of Symp. in Appl. Math. **51** (1995) *The Interface of Knots and Physics*, (L. H. Kauffman, ed.), Amer. Math. Soc., Providence, arXiv:q-alg/9607001. See pp. 24.

[BN2] D. Bar-Natan and others, *Caen Workshop on v- and w-Knotted Objects,* 2012 workshop in Caen. Videotaped lectures at `http://www.math.toronto.edu/~drorbn/Talks/Caen-1206/`. See pp. 39.

[BN3] D. Bar-Natan, *(u, v, and w knots)×(topology, combinatorics, low algebra, and high algebra),* 2013 master class in Aarhus. Videotaped lectures at `http://www.math.toronto.edu/~drorbn/Talks/Aarhus-1305/`. See pp. 39.

[BN4] D. Bar-Natan, *Balloons and Hoops and their Universal Finite Type Invariant, BF Theory, and an Ultimate Alexander Invariant,* Acta Mathematica Vietnamica **40-2** (2015) 271–329, arXiv:1308.1721. See pp. 39.

[BN5] D. Bar-Natan, *Over-then-Under-tangles and the Drinfel'd Double,* talk at *Expansions, Lie Algebras, and Invariants,* Workshop at CRM, Montreal, July 2019. Video at `http://drorbn.net/m19/#Bar-Natan-4`. See pp. 38.

[BN6] D. Bar-Natan, *Geography vs. Identity,* talk at the *CMS Winter 2019 Meeting,* in Toronto, December 2019. Handout and video at `http://drorbn.net/to19/#1`. See pp. 11.

[BN7] D. Bar-Natan, *Finite Type Invariants of W-Knotted Objects IV: Some Computations*, paper and related files at `http://drorbn.net/AcademicPensieve/Projects/WKO4`, arXiv:1511.05624. See pp. 39.

[BD1] D. Bar-Natan and Z. Dancso, *Finite Type Invariants of W-Knotted Objects I: W-Knots and the Alexander Polynomial,* Alg. and Geom. Top. **16-2** (2016) 1063–1133, arXiv:1405.1956. See pp. 39.

[BD2] D. Bar-Natan and Z. Dancso, *Finite Type Invariants of W-Knotted Objects II: Tangles and the Kashiwara-Vergne Problem,* Math. Ann. **367** (2017) 1517–1586, arXiv:1405.1955. See pp. 39.

[BD3] D. Bar-Natan and Z. Dancso, *Finite Type Invariants of W-Knotted Objects III: Double Tree Construction,* `http://drorbn.net/AcademicPensieve/Projects/WKO3` (in preparation). See pp. 39.

[BDV] D. Bar-Natan, Z. Dancso, and R. van der Veen, *Over then Under Tangles,* (self-reference), paper and related files at `http://drorbn.net/OU-JKTR`. The arXiv:2007.09828 edition may be older. See pp. 1, 27, 32, 33, 37.

[BM] D. Bar-Natan, S. Morrison, and others, `KnotThery‘`, a knot theory mathematica

package, http://katlas.org/wiki/The_Mathematica_Package_KnotTheory. See pp. 32.

[BCP] P. Bellingeri, B. A. Cisneros de la Cruz, and L. Paris, *A Simple Solution to the Word Problem for Virtual Braid Groups,* Pac. J. of Math. **283-2** (2016) 271–287, arXiv:1506.05283. See pp. 12.

[Be] G. M. Bergman, *The Diamond Lemma for Ring Theory,* Adv. in Math. **29-2** (1978) 178–218. See pp. 16.

[BB] J. S. Birman and T. E. Brendle, *Braids: A Survey,* in *Handbook of Knot Theory,* (W. Menasco, M. Thistlethwaite, eds.) Elsevier 2005, arXiv:math/0409205. See pp. 9.

[Ch1] O. Chterental, *Virtual Braids and Virtual Curve Diagrams,* J. of Knot Theory and its Ramifications **24-13** (2015), arXiv:1411.6313. See pp. 12, 22.

[Ch2] O. Chterental, *Virtual Braids and Virtual Curve Diagrams,* University of Toronto Ph.D. thesis, http://hdl.handle.net/1807/70904. See pp. 12, 22.

[En1] B. Enriquez, *On Some Universal Algebras Associated to the Category of Lie Bialgebras,* Adv. in Math. **164-1** (2001) 1–23, arXiv:math/0101059. See pp. 2, 39.

[En2] B. Enriquez, *A Cohomological Construction of Quantization Functors of Lie Bialgebras,* Adv. in Math. **197-2** (2005) 430–479, arXiv:math/0212325. See pp. 2, 39.

[Ep] D. B. A. Epstein and others, *Word Processing in Groups,* A. K. Peters, Natick, 1992. See pp. 32.

[EK] P. Etingof and D. Kazhdan, *Quantization of Lie Bialgebras, I,* Sel. Math. New Series **2** (1996) 1–41, arXiv:q-alg/9506005. See pp. 39.

[GP] E. Godelle and L. Paris, *$K(\pi, 1)$ and Word Problems for Infinite Type Artin-Tits Groups, and Applications to Virtual Braid Groups,* Math. Zeitschrift **272** (2010) 1339—1364, arXiv:1007.1365. See pp. 12.

[Ka1] L. H. Kauffman, *Virtual Knot Theory,* European J. Comb. **20** (1999) 663–690, arXiv:math.GT/9811028. See pp. 10.

[Ka2] L. H. Kauffman, *Rotational Virtual Knots and Quantum Link Invariants,* arXiv:1509.00578. See pp. 10, 25.

[Ma] V. O. Manturov, *Virtual Knots, The State of the Art,* Series on Knots and Everything **51**, World Scientific 2012. See pp. 10.

[Mi] J. W. Milnor, *Link Groups,* Annals of Math. **59** (1954) 177–195. See pp. 38.

[MV] J. Murakami and R. van der Veen, *Quantized $SL(2)$ Representations of Knot Groups,* arXiv:1812.09539. See pp. 25.

[Ne] M. H. A. Newman, *On Theories with a Combinatorial Definition of "Equivalence",* Ann. of Math. 2nd Ser. **43-2** (1942) 223–243. See pp. 17.

[Sa] M. V. Sapir, *Combinatorial Algebra: Syntax and Semantics,* Springer 2014. See pp. 16.

[Se] P. Ševera, *Quantization of Lie Bialgebras Revisited,* Sel. Math. New Series **22** (2016) 1563–1581, arXiv:1401.6164. See pp. 39.

[Sm] G. Smolka, *Confluence and Normalization in Reduction Systems,* Lecture Notes, 2015, https://www.ps.uni-saarland.de/courses/sem-ws15/ars.pdf. See pp. 16.

[Th] D. Thurston, Sutured Manifolds and Hopf algebras, talk at *Expansions, Lie Algebras, and Invariants,* Workshop at CRM, Montreal, July 2019. Video at http://drorbn.net/m19/#Thurston. See pp. 38.

[Wol] *Wolfram Language & System Documentation Center,* ωεβ/Wolf. See pp. 27.

[Wor] S. L. Woronowicz, *Solutions of the Braid Equations Related to a Hopf Algebra,* Lett. Math. Phys. **23** (1991) 143–145. See pp. 25.